This is a non-peer-reviewed preprint submitted to EarthArXiv.

This manuscript has been submitted for publication in Lithos. Please note the manuscript has yet to be formally accepted for publication. Subsequent versions of this manuscript may have slightly different content. If accepted, the final version of this manuscript will be available via the 'Peer-reviewed Publication DOI' link on the right-hand side of this webpage.

Platinum-Group Element systematics in the North Atlantic Igneous Province: new insights from Northern Irish and Irish magmatism

Anna O. Morrison[1], Michael J. Stock[1,*], Mark R. Cooper[2], Jens C. Ø. Andersen [3], Hannah S.R. Hughes[3], Elliot J. Carter[4], Jack Beckwith[1], Iain McDonald[5], Andrew C. Kerr[5], Paul Mohr[6]

[1]Discipline of Geology, School of Natural Sciences, Trinity College Dublin, Dublin, Ireland

[2]Geological Survey of Northern Ireland, Adelaide House, 39-49 Adelaide St., Belfast, UK

[3]Camborne School of Mines, University of Exeter, Falmouth, UK

[4]School of Life Science, Keele University, Keele, UK

[5]School of Earth and Environmental Sciences, Cardiff University, Cardiff, UK

[6] Department of Geology, University of Galway, Galway, Ireland

*Corresponding: Michael.Stock@tcd.ie

Key Words: North Atlantic Igneous Province, British and Irish Palaeogene Igneous Province, Icelandic plume, Platinum Group Elements, Dykes

ABSTRACT

The North Atlantic Igneous Province (NAIP) is one of the most prospective regions for Ni-Cu-Platinum-Group Element (PGE) mineralisation in Europe, and recent studies have discovered elevated PGE concentrations within its early lavas and minor intrusions comprising the British and Irish Palaeogene Igneous Province (BIPIP). This study presents an extended digital map of the regional mafic dyke swarms associated with the BIPIP in Northern Ireland and Ireland and a comprehensive new geochemical dataset of these magma conduits, the Antrim Lava Group and associated minor intrusions, including PGE and Au analyses. Digital mapping using

aerial electromagnetic data reveals a high density of dyke-related anomalies on the island of Ireland. Dyke density and orientation indicate at least one swarm originating from an onshore Palaeogene igneous centre (Slieve Gullion, Carlingford, possibly Dromore High), whilst others are likely propagating from submarine igneous centres in the North Atlantic. The origins and evolution of dyke swarms provide context for interpreting variations in PGE abundances. Previous authors have highlighted that early NAIP magmatic rocks (e.g., Greenland and Scotland) had high Pt/Pd ratios (~1.9), while younger sequences (e.g., Iceland) trend towards lower ratios (~0.4). Our data reveal that Irish BIPIP centres record a similar transition with an average Pt/Pd ratio of 1.6 ± 0.8, reflecting an evolving geodynamic setting where the magmatic conditions transitioned from intra-plate volcanism through to the inception of continental rifting and ocean opening. A close spatiotemporal association between variable Pt/Pd in BIPIP rocks in Ireland and high Pt/Pd in BIPIP rocks in Scotland suggests that the geodynamic transition occurred within a geologically short time interval (<1 Myr). Results from our samples attest to widespread sulphide saturation, supporting the potential for orthomagmatic Ni-Cu-PGE mineralisation within related central complexes or magmatic feeder networks.

HIGHLIGHTS

- Most Irish Palaeogene dykes originate from offshore North Atlantic igneous centres.
- The oldest Erne dykes may originate from onshore Irish central complexes.
- Irish Palaeogene magmatism records the earliest stages of North Atlantic opening.
- Pt/Pd ratios record a rapid geodynamic transition during North Atlantic rifting.
- Irish Palaeogene magmas have typically saturated in sulphide liquids.

1. Introduction

Platinum Group Elements (PGE) are useful proxies for mantle processes and geodynamic environment, in addition to being classed as critical raw materials, necessary to achieve climate

mitigation goals (Mudd et al., 2018). They are ubiquitously siderophilic (Barnes and Ripley, 2016) but can be divided into two groups with different geochemical behaviours: the Platinum group PGEs (PPGE; Pt, Pd and Rh) are mainly hosted in base metal sulphides, whilst the Iridium group PGEs (IPGE; Ir, Os, Ru) form alloys and monosulphide solid solutions (Maier and Groves, 2011; Barnes and Ripley, 2016). Recent studies have highlighted a close association between large igneous provinces (LIP) and PGE mineralisation (e.g., Norilsk-Talnakh, Bushveld; Maier, 2005; Barnes and Mansur, 2022) with LIP-related Ni-Cu-PGE deposits sharing geochemical characteristics that have been attributed to a metasomatic component from the sub-continental lithospheric mantle (SCLM; Griffin et al., 2013; Barnes et al., 2016), though the extent and significance of this contribution remain debated. It has been suggested to result from parental magmas intruded at cratonic edge blocks mobilising sulphides from enriched continental roots (Chen et al., 2025).

Early NAIP magmatism occurred under conditions conducive to PGE mineralisation (Andersen et al., 2000) and has been the subject of PGE exploration (e.g., Skaergaard, Kap Edvard Holm and Rum complex; Andersen et al., 2000; Hughes et al., 2015c; Andersen et al., 2017). Recent studies have shown that metal systematics in the British and Irish Palaeogene Igneous Province (BIPIP), an early manifestation of the NAIP (63-52 Ma; Musset et al., 1988), record contamination of plume-derived magmas by SCLM at margins of the North Atlantic Craton (Hughes et al., 2015b), resulting in enrichment of PPGEs. This pattern is consistent with major global PGE deposits where historic metasomatism during orogenic events can ‘precondition’ the cratonic SCLM, enriching it in Pt, and influencing the precious metal budget and Pt/Pd ratios of ascending magmas during LIP formation (Maier and Groves, 2011; Griffin et al., 2013). Furthermore, authors have suggested that the NAIP has a high primary PGE concentration in the mantle source, which is a critical prerequisite for orthomagmatic Ni–Cu–PGE mineralisation (Andersen et al., 2000).

Despite extensive work on the PGE potential and geodynamic evolution of the BIPIP, previous studies have relied strongly on the Hebridean portion of province, extrapolating results to Northern Ireland and Ireland (Hughes, 2015 and references therein); while the major element, trace element and isotopic geochemical behaviour of Northern Irish and Irish BIPIP rocks have been investigated (Mohr, 1988; Andersen et al., 2000; Carter et al., 2024), detailed studies of PGE systematics are sparse and largely limited to industry datasets (Hurst, 1997; Smyth, 2014). This study addresses this knowledge gap by first digitising Palaeogene regional dyke swarms on the island of Ireland using newly available aerial magnetic datasets and then presenting a new geochemical characterisation of these dykes, in addition to the Antrim Lava Group (ALG) and minor intrusions (sills and plugs), including PGE and Au concentrations. We use these data, alongside a literature data compilation, to constrain the mantle petrogenesis, S-saturation processes and PGE mineralisation potential during the evolution of the early NAIP.

2. Geological Setting

2.1. Overview of the North Atlantic Igneous Province

The NAIP includes volcanic and plutonic magmatism in Greenland, the Faeroe Islands, Britain, Northern Ireland, Ireland, Iceland and the surrounding offshore, which formed as a result of the (proto-) Icelandic plume impinging on the base of lithosphere (Fig. 1; Saunders et al., 1997), coupled with extension during North Atlantic rifting (Hansen et al., 2009; Wilkinson et al., 2016). Magmatic activity began in the Palaeogene in present-day western (e.g. Greenland) and eastern (e.g. Britain, Ireland) Atlantic, with ages broadly converging on modern day Iceland (Fig. 1). Palaeogene magmatism can be divided into two phases with a pre-rift phase at 62–58 Ma, followed by a hiatus at ~57 Ma, and a subsequent voluminous syn- and post-rifting phase coincided with the opening of the North Atlantic at ~56–53 Ma (Saunders et al., 1997;

Wilkinson et al., 2016). Plume-related volcanism has transitioned from continental to oceanic geodynamic settings throughout the last ~62 Myr (Hughes et al., 2015b).

2.2. The British and Irish Palaeogene Igneous Province in Ireland

Palaeogene igneous rocks in Britain and the island of Ireland comprise the BIPIP and include on- and offshore central igneous complexes, lava flows and regional dyke swarms (Fig. 2; Andersen et al., 2000; Kent and Fitton, 2000; Mitchell, 2004). Based on previous geochronological constraints, the first pulse of BIPIP magmatism occurred at ~61 Ma with the eruption of basaltic lavas into the Hebridean basin and the northeast of Ireland (Mussett et al., 1988; Cooper et al., 2012). The bulk of magmatic activity followed between ~61–59 Ma, marked by the emplacement of large mafic and silicic central complexes (e.g., Mull, Rum, Carlingford, and Slieve Gullion; Chambers and Pringle, 2001), widespread sills and dyke intrusion and effusive lava extrusions (e.g., Skye, Antrim). A second pulse of late-stage dyke emplacement continued until ~58 Ma (Mitchell, 2004). Recent work by Cooper et al. (2020, 2026) proposed a third pulse of activity at ~56–56.5 Ma, associated with emplacement of the Mourne Mountains. Analysing BIPIP samples, therefore, presents an opportunity to investigate petrogenetic changes through ~5.5 million years of geodynamically diverse magmatism (Fig. 3b) as the NAIP transitioned from a pre- to syn-rift phase (Saunders et al., 1997). Broadly contemporaneous with this onshore magmatism, offshore magmatism in the North Atlantic generated submarine igneous centres such as the Anton Dohrn, Hebrides Terrace and Blackstones Bank which have not been analysed extensively and are predominantly constrained by geophysical surveys or during dredging expeditions (Ritchie and Kitchen, 1996; O'Connor et al., 2000).

2.2.1. The Antrim Lava Group

The ALG (Fig. 2) is the most extensive extrusive suite in the BIPIP (59.4-61 Ma), comprising ~3,800 km^2 of flood basalts preserved in the northeast of Northern Ireland (Saunders et al., 1997, Mitchell, 2004). The lavas are separated into two stratigraphic sequences: the Upper (UBF) and Lower Basalt Formations (LBF), which each represent ~0.5 Ma of activity, separated by ~0.5 Ma of quiescence (Mitchell, 2004; Carter et al., 2024). The age of the LBF is well constrained between ~61.6 and ~61.1 Ma by U-Pb zircon ages from the underlying Clay with Flints and Tardree Rhyolite Complex (Cooper et al., 2026). The quiescent (interbasaltic) period is marked by thick laterites and only minor eruptive activity, which produced the Causeway Tholeiite Member (Fig. 3b; Lyle and Preston, 1993; Wilkinson et al., 2016). Recent studies have calculated that mantle potential temperatures varied significantly (T_p 1374–1521 °C) during ALG emplacement as a result of thermal pulsing in the (proto-) Icelandic plume (Carter et al., 2024).

2.2.2. Dyke Swarms

The BIPIP contains characteristic NW–SE dykes formed as a result of NE–SW extension during Palaeogene mantle plume activity (Geoffroy et al., 1996). Five swarms, dated between ~61–56 Ma (Cooper et al., 2026), traverse the island of Ireland (Cooper et al, 2012, Anderson et al., 2016, 2018), spatially and temporally overlapping the emplacement of three exposed onshore central complexes (Mournes, Carlingford, Slieve Gullion) as well as the ALG. The enigmatic Dromore High, a positive gravity anomaly within low-density Devonian and Carboniferous bedrock (Reay, 2004), likely represents a buried pluton also within the region of high-density dyke emplacement. It has been suggested to correspond to a Palaeogene igneous body analogous to the Slieve Gullion Complex (Mitchell, 2004; Shaw et al., 2022), though other interpretations, including a subsurface extension of the Ordovician Tyrone Igneous Complex, are also possible (Cooper et al., 2011; Anderson et al., 2018)

While only the Erne Dyke Swarm has an absolute age (Cooper et al., 2026), relative age constraints exist for other swarms (Fig. 3; Anderson et al., 2018). In decreasing age order: the oldest dykes comprise the Erne Dyke Swarm (61.34 ± 0.11 Ma) which is most abundant in the mid-west of the island of Ireland, along the Irish–Northern Irish border. The swarm has a low dyke density with a general WNW–ESE strike (Cooper et al., 2012). The second-oldest Donegal-Kingscourt Dyke Swarm is a high-density swarm, emplaced across the northwest to the southeast of Ireland, with a NW–SE strike (Anderson et al., 2018). Both the Erne and Donegal-Kingscourt swarms are truncated by the LBF (Cooper et al., 2026) suggesting that they may have contributed to extrusion of the ALG. Next, the Killala Dyke Swarm, which is younger than the Killala Gabbro (60.957 ±0.041 Ma; Cooper et al., 2026), propagates across the northwest of Ireland with a W–E strike, contrasting with the general BIPIP dyke trend (NW–SE; Geoffroy et al., 1996). Killala dykes occur in a lower density than Donegal-Kingscourt but a comparatively smaller area within the limits of the Tellus geophysical dataset of the time (Anderson et al., 2018). The NE-SW striking West Connacht (Mohr, 1988) and N-S striking Dingle dykes (Morris, 1974) outcrop with low densities on the west and southwest coast of Ireland, respectively, again contrasting with the general BIPIP dyke orientation. These have not previously been mapped using Tellus aeromagnetic data because prior studies were conducted before completion of the survey in those areas (Anderson et al., 2016, 2018) but lithological and magnetic data support a Palaeogene age (Mussett et al., 1988). The Ardglass-Ballycastle swarm strikes NW–SE on the east coast and cross-cuts the LBF but generally not UBF, constraining their formation to the interbasaltic period between 59.9–60.5 Ma (Fig. 3; Cooper et al., 2012; Anderson et al., 2018). Finally, the high-density, NW–SE striking St. John's Point Lisburn swarm also occurs on the east coast of the island and cuts both the LBF and UBF, indicating intrusion after 59.4 Ma (Fig. 3b; Anderson et al., 2018).

2.2.3. Sills and Plugs

Northern Ireland is host to many doleritic and gabbroic sills, with intrusions beneath and within the ALG (Mitchel, 2004; Holness et al., 2025). In County Antrim, the Portrush Sill has been dated at 58.453 ± 0.029 Ma (Cooper et al., 2026), whilst in County Down, the Scrabo Sill complex has been dated at 61.318 ±0.026 (i, Fig 3e; Cooper et al., 2026). Several doleritic plugs associated with the ALG represent sites of localised eruptive activity, with the Slemish plug representing the largest volcanic vent on the island of Ireland and outcropping on the Antrim Plateau (Preston, 1963; Mitchell, 2004).

2.2.4. PGE exploration in the Irish and Northern Irish BIPIP

The Carlingford Complex was subject to PGE exploration by BHP in the 1990s, sparked by the discovery of a 'float boulder' containing ~5 wt% Cu, 1.5 ppm Pt and 1.5 ppm Pd (Hurst, 1997). Following BHP's withdrawal from the area, Belmore Resources Ltd assumed the licence in 2005, finding further Pt mineralisation in dykes and several boulders containing mineralised PGE ± Au, Ni and Cu (Goodman and Slowley, 2005). Further potential for PGE mineralisation in Northern Ireland and Ireland was highlighted by the Tellus regional exploration programme (see Supplementary Text for references to national datasets) which identified significant Pt and Pd anomalies in stream and soil sediment samples, particularly in northwest and east County Antrim, associated with the ALG and its feeder dykes (Lusty, 2016). These findings spurred exploration interest in the region, leading Lonmin Plc. to acquire exploration licences in the from 2008–2017 (Smyth, 2014; Lonmin Plc, 2018). More recently, Karelian Diamond Resources has expressed interest in Ni-Cu-PGE exploration in the southwest of Northern Ireland, following encouraging results in stream sampling campaigns (Karelian Diamond Resources, 2025).

3. MATERIALS AND METHODS

3.1. Digital mapping

New digital maps of dyke-related anomalies across Northern Ireland and Ireland were produced following the method of Cooper et al. (2012) and Anderson *et al.* (2016, 2018) but using a more complete aerial magnetic dataset extending across most of the island of Ireland (see Supplementary Text for references to national datasets), as opposed to only Northern Ireland and the border counties. Data from West Cork and Kerry are not shown on our map as Tellus datasets were not available at the time of this study. We used a free-to-access, pre-processed geoTIFF of First Vertical Derivative of the Reduced to Pole Total Magnetic Intensity anomaly field to constrain the locations of dyke-related features. Dyke-related anomalies were digitised in QGIS by tracing linear magnetic anomalies and classified into swarms based on orientation and location, creating an extended database of georeferenced polylines. At the current resolution (grid cell size 35m), individual dyke-related anomalies may reflect the cumulative effect of multiple overlapping dykes rather than a single outcropping dyke. This means that the number of intrusions is likely to be much greater than the number of mapped anomalies but may not reflect outcrop exposure. The digital mapping exercise has not yet been extensively tested on the ground, however, some western dykes have been identified during fieldwork for sample collection.

3.2. Sample collection and preparation

Samples of putative magmatic 'liquids' (i.e. lavas and dykes, rather than cumulates) were collected from across the island of Ireland for geochemical analysis (Table 1). They were collected in multiple field campaigns and analysed in multiple laboratories which we describe in three methodological subgroups. Dykes, sills and plugs were collected by the Geological Survey of Northern Ireland during multiple field campaigns in 2013–2014 study (subgroup A). Dyke samples from the west coast of Ireland and Carlingford cone sheets were collected during fieldwork in June 2024 and August 2022, respectively, specifically targeting finer-grained dyke margins (subgroup B). Sills (e.g., Portrush, Magilligan), plug (e.g., Slemish) and cone sheet

samples from Subgroups A and B comprise ‘minor intrusions’ within this study. Antrim lava samples were collected from boreholes drilled by Lonmin Plc. across Northern Ireland in 2013 (subgroup C), focused on the lowermost (first) flow in drill cores (Lower Basalt Formation). Lavas constitute extrusive samples within this study. In hand specimen, samples were either crystal-free or porphyritic with a glassy or microcrystalline groundmass and occasional phenocrysts of olivine and/or clinopyroxene. Plagioclase was rarely present, and opaque (presumably oxide) phases were visible in thin section.

Samples from subgroups A and C were similarly powdered at the Centre for Environmental Geochemistry, Nottingham, and the School of Earth and Environmental Sciences, Cardiff University, respectively. Samples from subgroup B were prepared in the Discipline of Geology, Trinity College Dublin, first removing weathered material from the edge of each sample and washing in deionised water, before crushing in a tungsten carbide jaw crusher and grinding to a fine powder in an agate mill. If present, amygdales and filled vesicles were hand-picked and removed from crushed samples.

3.2. Major and trace element analysis

Loss on Ignition (LOI) was measured gravimetrically for subgroups A and B by heating powders (2g) at 1000°C for one hour. For subgroup C, LOI was measured using ~1.5 ± 0.0001g of sample powder baked at 900°C in a Vecstar Furnace for 2 hours. Total sulphur for subgroup B was measured using an Analytik Jena multi-EA 40000 instrument in the Earth Surface Research Laboratory, Trinity College Dublin. Accuracy and precision were ~10% and ~2%, respectively, from repeat analysis of reference material 2648c (Table S1).

Samples from subgroup A were analysed in the Centre for Environmental Geochemistry, Nottingham (Table 2), with major element concentrations measured on fused beads by Panalytical Zetium Wavelength Dispersive-Xray Florescence (WD-XRF) spectroscopy and

trace elements by Agilent 7500 Ionising Coupled Plasma-Mass Spectroscopy (ICP-MS) following sodium peroxide fusion after Hollis et al. (2015). Analytical uncertainties for trace elements were assessed using BCR-2 certified reference material; while major elements uncertainties were monitored by repeat analysis of JG1a, JG3, BE-N, GXR-1. The major element compositions of subgroup B were analysed on fused glass beads using a Panalytical Zetium WD-XRF in the Malvern Panalytical Laboratory, Nottingham, while the trace element compositions of subgroup B were analysed on pressed powder pellets using a Panalytical Zetium WD-XRF instrument in the Earth Surface Research Laboratory, Trinity College Dublin. Samples were prepared and analysed following Carter et al. (2024). Analytical uncertainties were constrained using certified reference materials GSJ JB-1b, JB-3a and JBb-1 for major elements and GSJ JA-1a, JA-2 and JB-2 for trace elements. Subgroup C was analysed in the School of Earth and Environmental Sciences, Cardiff University. Major elements, minor elements and Sc were measured using a JY-Horiba Ultima 2 Inductively Coupled Plasma Optical Emission Spectrometry (ICP-OES) and trace elements were measured using a thermoelemental X series (X7) ICP-MS, following McDonald and Viljoen (2006). Standard reference materials JB1a, JP1 and MRG1 were used to constrain uncertainties. Representative accuracy for major elements is typically 1–2%, except for Na_2O (3%) and P_2O_5 (4%). Representative accuracy for trace elements is typically 5–8%, except Zr (20%) and Ba (33%; see Supplementary Text for full certified reference material references).

3.3. PGE + Au fire assay

Platinum-Group element and Au concentrations for subgroups A and B were analysed at Activation Laboratories Ltd, Canada, by Ni-sulphide fire assay followed by ELAN 9000 ICP-MS, following Hoffman and Dunn (2002). Subgroup C was also analysed for PGE + Au by Fire Assay and thermoelemental X7 ICP-MS in the School of Earth and Environmental Sciences, Cardiff University, following Huber et al. (2001). Analytical and preparation

accuracy and reproducibility (including potential nugget effects) were assessed following a validation approach similar to Passmore (2009; Table S2). Across all laboratories, representative accuracy for PGEs ± Au was between ~0.5– 9% (Pt 4%, Pd 6%). Precision for subgroups A and B was better than 5%, based on repeat analysis of standards AMIS 0498 and OREAS 13b, with potential nugget effects determined to be minor (Table S2).

4. A REVISED PALAEOGENE DYKE MAP

Our enhanced digital mapping of regional dyke swarms reveals a greater density of dyke-related anomalies than previously identified in the northwest and west of the island of Ireland and across the Irish Sea (Fig. 3a). Specifically, our new results build on the mapping of Cooper et al. (2012) and Anderson et al. (2016, 2018), extending the mapped geographic coverage of the Donegal-Kingscourt, Killala and Erne swarms in the west and northwest. The Fleetwood dyke swarm, initially thought as an offshore component of the Donegal-Kingscourt swarm (Anderson et al., 2018), has been mapped to strike WNW–ESE, with a low onshore density in the east, extending to a high-density swarm across the Irish Sea Basin and outcropping on the Isle of Man; the dykes crosscut early granites of the Mournes relatively constraining their age to ~56–56.5 Ma (Cooper et al., 2026). By mapping offshore continuations of the Donegal-Kingscourt, Ardglass-Ballycastle, St. John's Point, Lisburn and Fleetwood swarms, we provide new insights into the high density of dyke-related anomalies in the Irish Sea, demonstrating that the Fleetwood and Ardglass-Ballycastle swarms transect the Isle of Man.

In addition, we identify and map a dyke swarm which was not previously recognised in aerial magnetic studies by Anderson et al. (2016, 2018): the West Connacht dykes, originally mapped by Mohr (1988), comprise a high-density swarm with a NE–SW strike inland transitioning to more W–E on the western coast. They have a much higher density than previously identified in outcrop by Mohr (1988), occurring in clusters along the west coast, with fewer dykes inland.

The West Connacht swarm shares orientation (W–E) with the Killala swarm on the northwest coast, however, their northern extent does not overlap inland with the Killala dykes. The Dingle dyke swarm mapped by Morris (1974) has not yet been resolved in our dataset due to incomplete Tellus survey data for the area.

The orientation of dyke swarms across the island of Ireland suggests a systematic regional variation, shifting from NW–SE in the north to predominantly W–E towards the southern extent of dyke propagation. Previous studies have suggested individual swarms have distinct strikes and that this shift in orientation reflects a temporal progression as a result of changing regional crustal stresses during north Atlantic opening (Anderson et al., 2018). However, our extended mapping demonstrates that some swarms are not continuous linear features with a constant strike but rather exhibit a pronounced curvature across their length, producing 'hockey stick' shaped regional features. This systematic change is exemplified by the St John's Point Lisburn dykes which have a NW–SE strike in the north but reorientate to a WNW–ESE strike in the south, across the Irish Sea and reach the Isle of Man. A similar re-orientation is observed in the West Connacht swarm, where more northernly dykes strike NE–SW while southern coastal dykes trend towards W–E.

5. GEOCHEMICAL RESULTS

For context, we compare our new geochemical results with those obtained for genetically related lava flows in Northern Ireland (Carter et al., 2024), the Scottish Hebrides (Hughes et al., 2015c), off- and on-shore East Greenland (Philip et al., 2001; Momme et al., 2002), West Greenland (Lightfoot et al., 1997; Keays and Lightfoot, 2007) and Iceland (Momme et al., 2003). This allows tracking North Atlantic plume dynamics from the Palaeogene to the present. Major and trace element results for all dykes, minor intrusions and lava flows are provided in

Table S3 and S4 and PGE+ Au results are in Table S5. Subgroups A and B comprise dykes and minor intrusions and subgroup C comprise Antrim Lava Group (ALG).

5.1. Major and lithophile trace elements

The major element compositions of our samples are broadly basaltic (Fig. S1; Alkali-subalkali basalts, tephrites), extending to highly primitive mantle-like compositions (>60 Mg#; Mg# = molar Mg/(Mg+Fe_t) x 100 where Fe_t = total Fe^{2+} + Fe^{3+}). However, two samples from the Dingle dyke system are highly evolved (dacite/rhyolite; Fig. S1), compared to other Northern Irish and Irish samples. The compositions of intrusive rocks and ALG samples overlap with dykes and minor intrusions, extending to slightly more evolved compositions; individual dyke swarms do not exhibit any observable geochemical difference with broadly similar major and trace element signatures across all swarms (Figs S2, S3). Compositional trends are consistent with fractional crystallisation of a mineral assemblage comprising predominantly olivine ± clinopyroxene ± minor plagioclase (Fig. 4a-d), as in other NAIP igneous centres (Lightfoot et al., 1997; Saunders et al., 1998; Kerr et al., 1999; Carter et al., 2024). While samples from Greenlandic centres have accumulated significant olivine (Fig. 4a) with high Mg content (>70 Mg#)and Fe_2concentrations (~13 O_3 concentrations (~13 wt%), our samples show less extensive olivine accumulation, extending to 50–70 Mg# and 10–14 % Fe_2. O_3. Olivine is consistently the liquidus phase in our samples, but the major element compositions indicate early clinopyroxene saturation (~55-60 Mg#), marked by an inflection in CaO concentrations with decreasing Mg#. None of our samples, and few NAIP literature analyses, show evidence of plagioclase saturation (which would be manifest as a decrease in Al_2O_3 at low Mg#). Lithophile trace elements (e.g. Zr and Sr) further support major element trends, with concentrations of incompatible elements increasing with decreasing Mg# (Fig. S4). The total

sulphur concentrations in our samples are low (average 0.13 wt%), consistent with an absence of visible sulphides in hand specimen (Table S1).

5.2. Chalcophile trace elements

The highest Ni, Cr and Co concentrations in our dataset are associated with the most mafic samples, with concentrations in all dyke and minor intrusion samples and most ALG samples decreasing at lower Mg# (Fig. 5). This mirrors data from other NAIP centres and is consistent with the 'incompatible fractionation' trend of Hughes et al (2015b), reflecting Ni and Co partitioning into olivine during progressive crystallisation, and Cr into presumably minor amounts of spinel-group minerals which are not apparent from major element variations (Fig. 4). A subset of ALG samples have lower Ni than the general trend for their given Mg# (Fig. 5a), reflecting early sulphide depletion before extensive crystallisation and sulphur saturation, as identified in some samples from West Greenland (Hughes et al., 2015).

As Cu is incompatible in common basaltic silicate minerals it increases in silicate melts as these phases crystallise (i.e., towards lower Mg#). If a sulphide liquid exsolves, however, Cu partitions strongly into this phase and decreases in the residual silicate melt. Both incompatible and compatible Cu trends are seen in the NAIP with sulphide-undersaturated crystallisation apparent from some Greenlandic samples and sulphide-saturated crystallisation dominant elsewhere (Hughes et al., 2015; Fig. 5d). Most of our data show decreasing Cu abundance with decreasing Mg#, consistent with magma being S-saturated (e.g. following trends in Scottish samples). However, a small number of our mafic ALG samples and one sill (Scrabo Sill; i, Fig. 3e) have anomalously high Cu relative to other samples at equivalent Mg#; this 'high Cu group' is consistent with sulphide-undersaturated crystallisation (Fig. 5d).

5.3. Platinum-Group elements and gold

Our samples contain negligible IPGE but PPGEs ± Au are generally above detection limit; Table S5). The highest total PGE concentration in our sample set is 34 ppb in an ALG sample, with the highest intrusive sample (a dyke from the Killala swarm) containing 28 ppb. The highest Pt concentration is 13 ppb and Pd 12 ppb, in the same dyke sample from the Killala swarm. The highest Au concentration is 26 ppb in an ALG sample. All other samples span the concentrations between these high values and the analytical detection limit. These concentrations are elevated relative to background mantle levels; average whole-rock MORB contains 0.5 ppb Pt and 0.9 ppb Pd (Hao et al., 2021).

Our data show similar systematics to the broader NAIP, with the highest and most variable Pt and Pd concentrations in the most mafic (highest Mg#) samples and lower concentrations in more evolved samples (Fig. 6a). Most of our samples have higher Pt than Pd concentrations. Only onshore East Greenlandic samples significantly deviate from this relationship, with high Pd even at low Mg#. Ruthenium concentrations are ubiquitously low, both in our samples (<4 ppb) and other NAIP centres (Fig. 6c). Similarly, Au concentrations are close to the detection limit and show do not correlate with Mg#; only onshore East Greenlandic centres and one of our samples from ALG (26 ppb) have higher concentrations.

The relationship between PGEs and other chalcophile elements can be used to identify their partitioning into immiscible sulphide liquids. For example, Cu and Pd are both incompatible in silicate minerals but partition strongly into sulphide liquids when magmas become S-saturated. Our data fall between two endmember trends in Cu versus Pd (Fig. 7a): one where Pd and Cu positively correlate up to ~15 ppb Pd and ~150 ppm Cu, and a second where Pd concentrations remain constantly low over a wide range of Cu abundances. The former trend is broadly consistent with other NAIP centre which show a general positive correlation between Cu and Pd, extending to the highest values and most variable concentrations in onshore East Greenland. The latter trend is more prominent in in group of samples from the ALG and a

single sill (subsequently denoted the ‘high Cu group’). Gold shows only a weak correlation with Pd in most of our samples (Fig. 7b), with slightly diverse populations between the ALG and intrusive samples, again consistent with the general NAIP trend except East Greenland which has higher and more scattered Au and Pd abundances.

While both Cu and Pd are chalcophilic, there is approximately an order of magnitude difference in their silicate melt–sulphide liquid partition coefficients, with Pd partitioning more strongly into the sulphide phase; Cu/Pd ratios of residual silicate melts therefore increase following S-saturation (Hughes et al., 2015c). The Cu/Pd ratios of mineralised PGE deposits tend to be lower than mantle values as they have not yet segregated sulphides and can concentrate PGE (Barnes et al., 1993, 2004, 2015); the extent of enrichment is enhanced through further silicate-magma interaction, with higher R-factors representing a greater volume of silicate magma interacting with sulphide, upgrading the sulphide tenor through additional PGE scavenging (Maier, 2005; Barnes et al., 2016; Lindsay et al., 2018). In contrast, magmas which have segregated sulphides have Cu/Pd ratios greater than mantle values as PGEs are preferentially lost (Barnes et al., 1993, 2004, 2015). The Cu/Pd ratios of our samples generally increase linearly with decreasing Pd concentration, and plot significantly above mantle values consistent with other NAIP centres (Fig. 8). Only the ‘high Cu group’ of samples plot slightly above the main data array.

As with major elements, there is little observable difference between our dyke, minor intrusion samples and ALG samples (or between dyke swarms) in terms of chalcophile elements, PGEs and Au, except that ALG samples extend to the highest Cu/Pd ratios.

5. DISCUSSION

5.1 Dyke origins

Of the seven mapped swarms, six show no obvious association with the onshore Palaeogene

central complexes of Slieve Gullion, Carlingford or the Mourne Mountains; they do not radiate from or curve towards these centres (e.g. as with the Mull swarm in southern Scotland and northern England; MacDonald et al., 2018**)** and in some cases are reported to crosscut them (Beckwith et al., 2026; Cooper et al., 2026). Irish dykes are also too far south to have originated from Hebridean Palaeogene centres (Mull, Rum, Skye; Fig. 2); their NW–SE strike would not intersect these intrusions. Figure 3a projects the offshore trajectories of dyke swarms from the north and west coasts of the island, assuming a constant strike. Dykes extending off the north coast (St. John's Point Lisburn) trend towards the Blackstones Bank complex, while dykes extending off the northwest coast (Donegal-Kingscourt) strike towards Anton Dohrn and the Hebrides Terrace (as previously identified by Ritchie and Kitchen, 1996). At larger map scales, these dykes appear to deflect close to the northwest coast as they intersect strike-slip faults (Fig. 3b). Our new mapping of the Killala and West Connacht swarms indicates that the predominantly W–E orientation of the coastal dykes does not align well with any offshore centre, including the more southern Brendan Igneous Centre (Figs. 2, 3) which has previously been suggested as the source of these intrusions (unless they reorientate dramatically offshore; Mohr 1982; Dewey 2000). Rather than originating from onshore Palaeogene centres, we suggest that most Palaeogene dyke swarms transecting the island of Ireland originate from offshore centres in the North Atlantic.

Existing age constraints support most dykes originating from offshore centres. The Donegal-Kingscourt swarm are relatively dated as being older than 61.4 Ma (early Palaeogene) owing to their being unconformably overlain by the LBF (Zircon U-Pb geochronology; Cooper et al., 2026), with an extended period of episodic volcanism at Anton Dohrn and the Hebrides Terrace between 70.4 Ma and 42.0 Ma (^{40}Ar–^{39}Ar; O'Connor et al., 2000). The St. John's Point Lisburn swarm (56–58 Ma) agrees well with dating of the Blackstones Bank dated at 58.6 ± 1 Ma (Pb

isotopes; Dickin and Durant, 2002).

The Erne swarm is an exception as its orientation does not trend towards any known offshore centre. From detailed inspection of our new aerial magnetic map, we suggest that these dykes, which have previously been grouped into a single swarm, in fact comprise two discrete populations: the Northern Erne sub-swarm with a NW–SE strike (similar to but slightly offset from the Donegal-Kingscourt dykes; light orange in Fig. 3a) and the Southern Erne sub-swarm with a more WNW–ESE strike (dark orange in Fig. 3a). The Southern Erne sub-swarm extends across the width of the island of Ireland but reorientates in the east, swinging towards and radiating from the Slieve Gullion and Carlingford central complexes (Fig. 3c) which have a near-contemporaneous age relationship with the Erne dykes (Cooper et al., 2012; Fig. 3e). In contrast, the Northern Erne sub-swarm has a notably high density proximal to the Dromore High gravity anomaly and do not extend more than 50 km southeast or northwest of this feature (Fig. 3d). While a component of the Dromore anomaly is thought to belong to Late Caledonian magmatism (Shaw et al., 2022), the possibility of a coincident Palaeogene central complex has not been discounted. The density of our mapped Northern Erne dykes supports the occurrence of Palaeogene magmatism in the Dromore area feeding these dykes. Hence, in contrast with other dykes which strike towards offshore NAIP igneous centres, we suggest that the Erne swarm may uniquely originate from onshore central complexes on the island of Ireland.

Recent work has also suggested that the Irish Sea experienced significant lithospheric thinning during the Palaeogene through uplift and magmatism caused by magmatic underplating (Bonadio et al., 2025). A thinned lithosphere may have accomodated propagating dykes more easily owing to the high density of intrusions identified in the Irish Sea basin (Fleetwood, St. John's Point Lisburn and Ardglass-Ballycastle dyke swarms).

5.2 Crystalisation and S-saturation in Northern Irish and Irish Palaeogene magmas

Our new geochemical results provide insights into Palaeogene magmatic processes during early lithospheric impingement of the proto-Icelandic plume and North Atlantic Rifting. Samples follow a typical tholeiitic fractional crystallisation trend with the liquid line of descent controlled predominantly by olivine ± clinopyroxene crystallisation with only minor late-stage plagioclase (Fig. 4a-d), consistent with previous studies of the BIPIP (e.g. Carter et al, 2024). Olivine crystallisation progressively depleted the residual melts in chalcophile Ni and Cr during magma evolution (Fig. 5a), with Co concentrations decreasing through the fractionation of spinel-group minerals.

The highest Pt, Pd and Ru concentrations are at high Mg# with lower concentrations in more evolved magmas, mirroring general trends in the NAIP and broadly consistent with PGE partitioning into sulphide liquids which progressively exsolve during magma evolution (Fig. 6a-c). However, there is a significant range in PGE concentrations at any given Mg# (Fig. 6a-d), suggesting heterogeneity in magmatic fractionation and S-saturation histories which exerts a primary control on magma chalcophile budgets.

While Naldrett (1999) suggested that whole-rock Ni concentrations as a Ni-Cu-PGE exploration vector, Barnes et al. (1993) highlight that other chalcophiles (e.g. Cu, PGEs) have much higher partition coefficients into sulphide liquids and are therefore more sensitive to S-saturation. Copper, for example, shows a continuous depletion in most of our data, consistent with sulphide saturation early in magmatic evolution and mirroring trends in most other NAIP centres, particularly Scotland. Only samples our 'high Cu group', comprising samples from the ALG and Scrabo Sill, have higher Cu concentrations consistent with incompatible behaviour during crystallisation of silicate minerals in the absence of sulphides and recording an absence of S-saturation (Fig. 5d). These samples represent some of the oldest samples in this study; Scrabo sill has been dated to 61.318 ± 0.026 Ma and falls within the estimated age range of the LBF which was erupted between 61.6 and 61.1 Ma (Fig. 3b; Cooper et al., 2026). Rather than

reflecting Cu enrichment by simple silicate fractional crystallisation, the ‘high Cu’ indicate the presence of minor disseminated chalcopyrite, implying that these samples sit within or adjacent to a mineralised system or area. This interpretation is consistent with chalcopyrite-bearing orthomagmatic sulphide assemblages described at the margin of the Skaergaard intrusion (Andersen et al., 2017). The low Pd contents of the ‘high Cu group’ (Fig. 7a) are consistent with early sulphide saturation that removed Pd from the silicate melt, followed by local separation and retention of a Cu-rich sulphide liquid. The subsequent magmatic evolution appears to have continued under sulphide-undersaturated conditions, such that the samples do not follow a typical sulphide-depletion trend (Fig. 5d).

The sulphur saturation history of a magma is critical to determining its orthomagmatic Ni-Cu-PGE sulphide mineralisation potential; the timing and mechanism of S-saturation are critical for deposit formation. In this study, the analysed lavas are interpreted as residual liquid compositions that had already experienced fractional crystallisation and attained S saturation prior to eruption. Consistent with this, whole-rock Cu/Pd ratios indicate that the melts had undergone sulphide segregation and are therefore chalcophile depleted, comparable with patterns reported from other NAIP centres (Fig. 8). As these sulphides are no longer associated with the magma (i.e. our samples are not sulphide-rich), they must have segregated from the melt, either within central complexes (e.g., Bushveld; Barnes et al., 2004) or conduit systems during crustal magma transport (e.g., Norilsk; Barnes et al., 2016), conducive to deposit formation. Mineralisation has previously been identified in Carlingford, both within the central layered complex and associated dykes (Goodman and Slowley, 2005; Beckwith et al., 2026), and positive mineralisation indicators have been identified in Northern Irish and Palaeogene dykes (Lusty, 2016; Group Eleven Corp., 2020). A key exploration challenge will be identifying any zones of localised sulphide accumulation, for example fluid dynamical traps (Barnes et al., 2016; Hughes et al., 2016) within the dyke systems which extend across the island of Ireland

(Dewey, 2000; Cooper et al., 2012; Anderson et al., 2016, 2018). Zones where dykes deflect across major faults (Fig. 3b) could provide such traps, as could areas proximal to the Dromore High, where conduits appear to be ascending near-vertically towards the surface; this is corroborated by soil compositions analysed in the Tellus geochemical survey which show elevated PGE concentrations associated with heavily faulted terranes and surrounding the Dromore High and along the northwest coast (Fig. 9).

5.3 Mantle dynamics recorded in the Northern Irish and Irish NAIP

Almost all of our samples only contain detectable PPGEs, with IPGEs largely below detection limits (>1ppb; subgroups A and B). This disparity may reflect the higher compatibility of IPGE in mantle sulphide phases, particularly monosulphide solid solutions, which preferentially retain IPGEs during partial melting (Maier, 2005; Singh et al., 2018). In addition, any subsequent sulphide saturation in the crust may depress total PGE without removing the PPGE/IPGE signature. Consequently, the following interpretations focus on PGE ratios rather than absolute concentrations within the samples.The Pt/Pd ratios of mafic melts preserve a record of geodynamic environment and mantle source conditions during magma generation (Hughes et al., 2015c; Lindsay et al., 2021). In the NAIP, Pt/Pd ratios generally decrease from high, near chondritic values in older igneous centres (~1.9; West Greenland ~63 Ma and Scotland ~61 Ma) to lower values in younger centres (~0.4; Iceland <50 Ma; Fig. 10a; Lindsay et al., 2021). This variation has been suggested to reflect transient mantle conditions associated with the opening of the North Atlantic. Higher Pt/Pd ratios are interpreted to reflect pre-rift, intraplate magmatism at the inception of the proto-Icelandic mantle plume and proximity to the North Atlantic Craton, whereas lower Pt/Pd ratios are suggested to record contributions from shallower mantle sources syn- and post-rifting of the Eurasian and North American plates (Griffin et al., 2013; Hughes et al., 2015c). Furthermore, the proximity of magma generation to cratonic boundaries impacts the PGE ratios of primary magmas (Griffin et al., 2013; Hughes

et al., 2015c; Lindsay et al., 2021) with higher Pt/Pd ratios in older NAIP centres thought to record partial melting of the SCLM at the margin of the North Atlantic Craton and lower ratios in younger centres recording the absence of a SCLM component (pre-rift). For example, Hebridean magmas generated close to the cratonic keel have had more opportunity to incorporate metasomatised Pt-enriched components within ascending magmas (Hughes et al., 2015c; Lindsay et al., 2021).

The Pt/Pd ratios of our samples range 0.4–5.04 with an average of 1.6 (Fig. 10a), spanning the range between older and younger NAIP centres reported in the literature data. There is structure within our dataset: older samples which formed before/during eruption of the LBF (61.6-61.1 Ma) have higher Pt/Pd ratios of ~1.85 (comparable to the Greenlandic and Scottish NAIP), whereas younger samples which formed during/after eruption of the UBF have a lower average Pt/Pd ratios of ~0.87 (comparable to offshore East Greenland; Fig. 10b;), trending towards modern Iceland. Our data record the disappearance of the SCLM component in primary melts between the LBF and UBF emplacement. The interbasaltic period between eruption of these basaltic formations marks a ~0.5 Myr near-hiatus in volcanic activity and correspond with a stabilisation and step-wise cooling of the proto-Icelandic plume (Fig. 10b; Cooper et al., 2020; Carter et al. 2024); we suggest that this period marks a major geodynamic transition from intraplate plume-dominated magma generation towards oceanic rifting-controlled petrogenesis (syn-rift). The time window between our oldest (e.g. LBF, Erne dykes, Donegal-Kingscourt dykes) and youngest (e.g. Fleetwood and St. John's Point Lisburn dykes) samples spans ~6 Myr (Fig. 3e; Cooper et al., 2026) which is comparable to the timescales inferred for the geochemical transition between West and East Greenland (Lindsay et al., 2021). Within this broader interval, our new data indicate that the critical transition from pre-rift SCLM-influenced magma generation to syn-rift melting that appears to have occurred during the

interbasaltic period (<1 Myr), highlighting transitional mantle conditions over a geologically short timescale (Fig. 3e, Fig. 10b).

6. CONCLUSIONS

Analysis of igneous centres on the island of Ireland provides new insights into precious metal behaviour and petrogenesis during a crucial phase of NAIP development. Our new digital maps show the distribution of seven discrete dyke swarms across Northern Ireland and Ireland, demonstrating that some swarms originate from submarine centres in the North Atlantic but that the Erne dykes likely derive from onshore centres; a Southern Erne sub-swarm appears to originate from the Slieve Gullion and Carlingford central complexes, while a Northern Erne sub-swarm is concentrated around the Dromore High gravity anomaly suggesting sub-surface Palaeogene magmatism. The major element compositions of our dykes, minor intrusions and lava samples are broadly consistent with other NAIP centres, with major elements controlled by olivine and clinopyroxene crystallisation and chalcophile trace elements recording persistent sulphide saturation, even in our most mafic magmas. The PGE concentrations of magmas feeding our samples are elevated relative to background mantle values and Pt/Pd ratios are highly variable, recording a changing geodynamic environment. Our work shows that older dyke swarms and related intrusive complexes, near contemporaneous with the LBF, have higher Pt/Pd ratios compared to younger rocks. The paucity of modern reliable isotopic ages prevents firm constraint of the younger dyke swarms and UBF, but they are likely to been emplaced <60.5 Ma. This transition records a major geodynamic shift in the interbasaltic period with older magmas recording plume-dominated melting and inclusion of a SCLM mantle component as a result of their proximity to the North Atlantic craton, and later magmas recording variable depletion and the absence of an SCLM component away from the cratonic margin. By integrating our results with existing absolute and relative dating of Northern Irish

and Irish igneous centres, we show that the transition from pre- to syn-rift environments in the NAIP occurred within a geologically short timeframe.

ACKNOWLEDGEMENTS

This work emanated from a Master's by Research grant co-funded by the Geological Survey of Ireland and the Northern Irish Department of the Economy, a Trinity College Dublin Foundation Scholarship, and research jointly funded by Taighde Éireann – Research Ireland and Geological Survey Ireland under grant number 20/FFP-P/8895. XRF data collection was supported by the Geological Survey Ireland-funded Earth Surface Research Laboratory in Trinity College Dublin. Maura Morgan and Sarah Carty are thanked for their assistance in sample preparation, and Hilde Koch, Clara Siqueira and Carmela Tupaz are thanked for their assistance in XRF sample preparation and analysis.

FIGURES

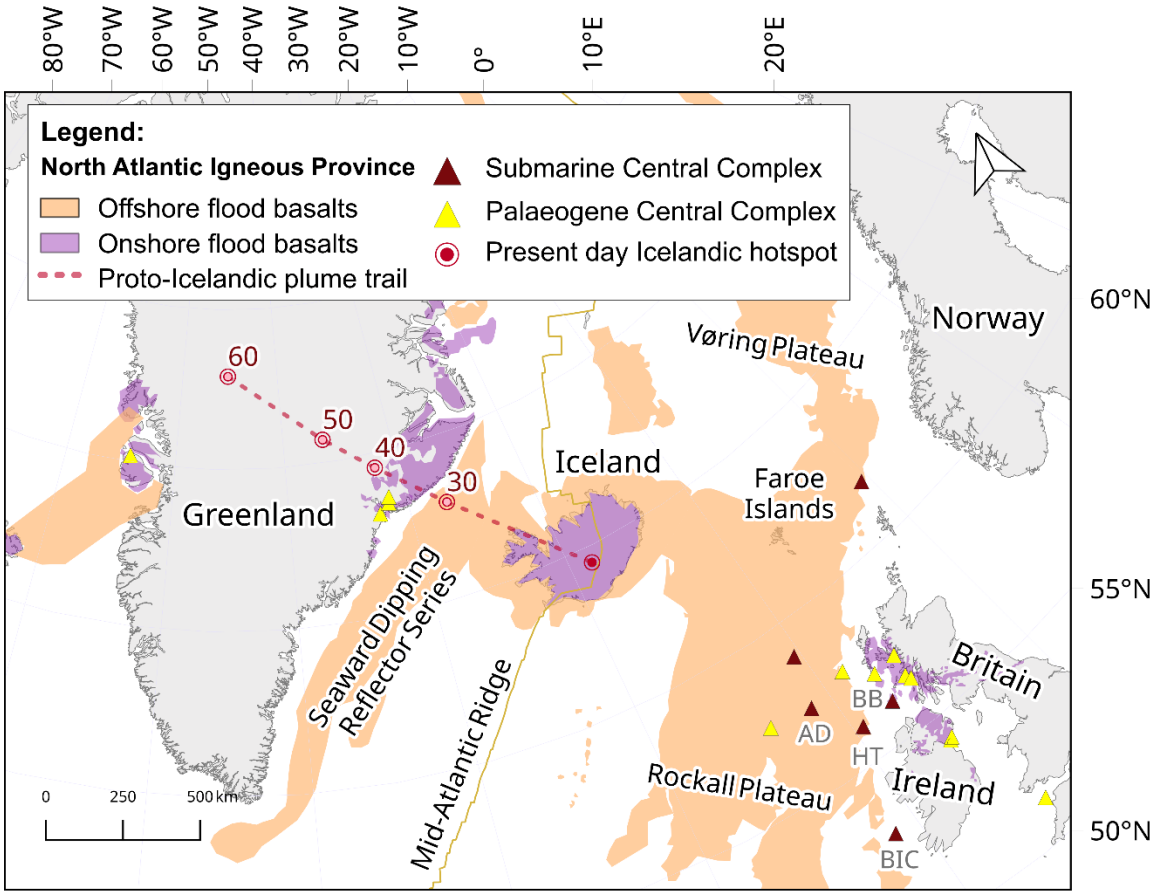

Figure 1: Simplified Geology of the NAIP, including onshore and offshore igneous centres and the hot-spot track of the proto-Icelandic mantle plume. Approximate ages of plume locations are given in red, leading to present-day Iceland. AD = Anton Dohrn, BB = Blackstones Bank, HT = Hebrides Terrace, BIC = Brendan Igneous Centre. Adapted from Mussett et al., 1988, Hughes et al., 2015c, Á Horni et al., 2017.

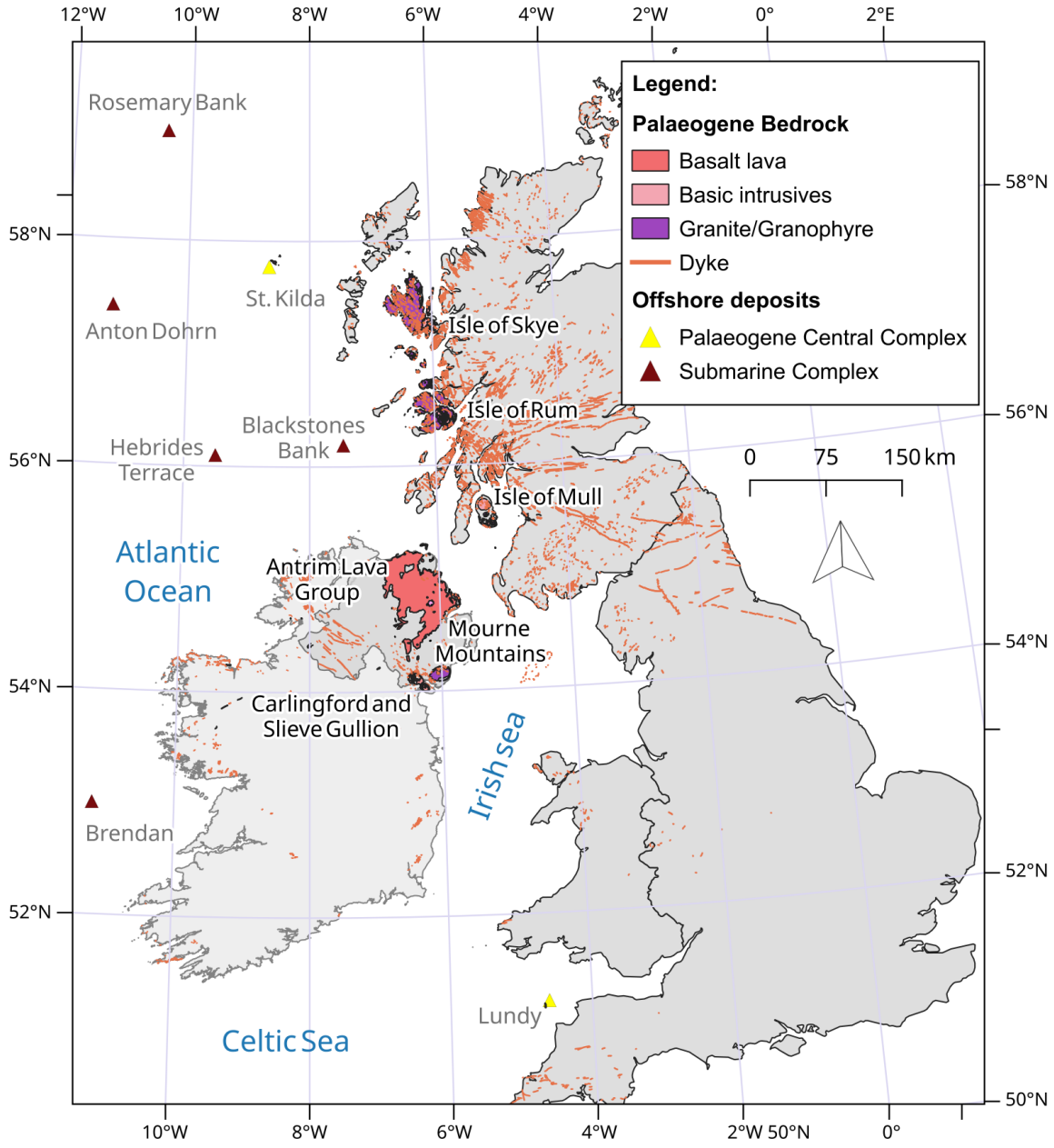

Figure 2: Simplified Regional Geology of the British and Irish Palaeogene Igneous Province. Dyke and igneous centre locations. See Supplementary Text for references to national bedrock geology dataset; offshore igneous centre locations from Mussett *et al.* (1988).

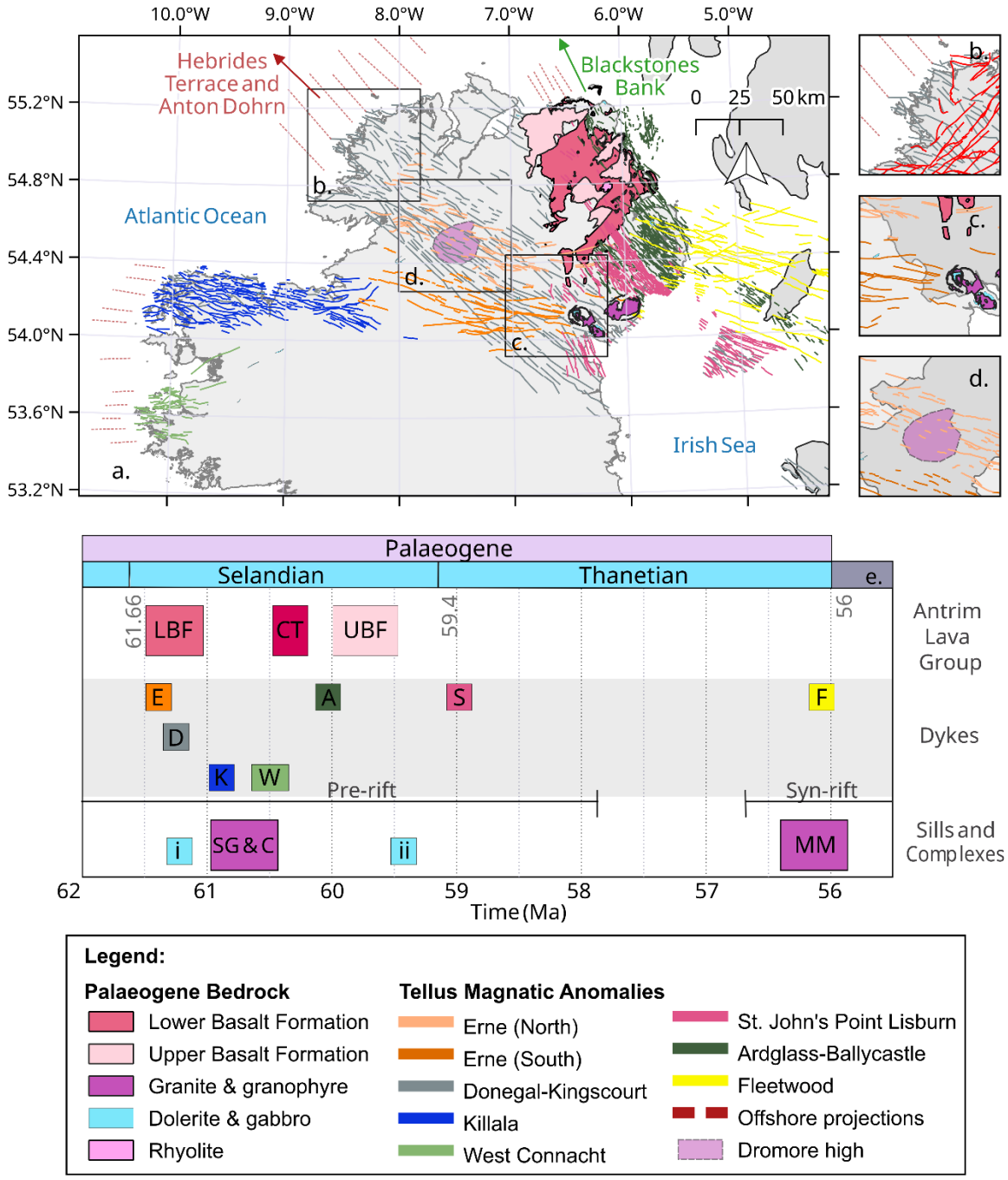

Figure 3: a) Results of extended BIPIP regional dyke swarm mapping in Northern Ireland, Ireland and associated offshore areas. Includes data from Anderson *et al.* (2016, 2018) with newly interpolated dyke extents from Tellus aerial magnetic data (see Supplementary Text for national Tellus datasets and bedrock data) and Bouguer anomaly from Mitchell (2004). Dashed lines indicate projected offshore dyke trajectories following onshore strikes. Arrows indicate

direction of offshore seamounts (see Fig. 2). Red arrow = towards Anton Dohrn and Hebrides Terrace, Green arrow = towards Blackstones Bank. Boxes show detailed regions: b) the northwest coast of Ireland where the Donegal–Kingscourt swarm intersects heavily faulted terrane and reorientates along coastal fault structures (in red), c) the area around Slieve Gullion and Carlingford where the Southern Earne sub-swarm reorient towards/radiate from the central igneous complexes, and d) the high-density Northern Erne sub-swarm proximal to the Dromore High. e) Overview stratigraphy of relative Palaeogene activity in Northern Ireland and Ireland, including data from Anderson et al. (2016, 2018) and Cooper et al. (2012, 2020, 2026). LBF = Lower Basalt Formation, CTF = Causeway Tholeiite Formation, UBF = Upper Basalt Formation, E = Erne Swarm, D = Donegal-Kingscourt Swarm, K = Killala Swarm, W = West Connacht Swarm, A = Ardglass-Ballycastle Swarm, S = St. Johns Point-Lisburn Swarm, F = Fleetwood Swarm, i = Scrabo Sill, ii = Portrush Sill, SG & C = Slieve Gullion and Carlingford MM = Mourne Mountains.

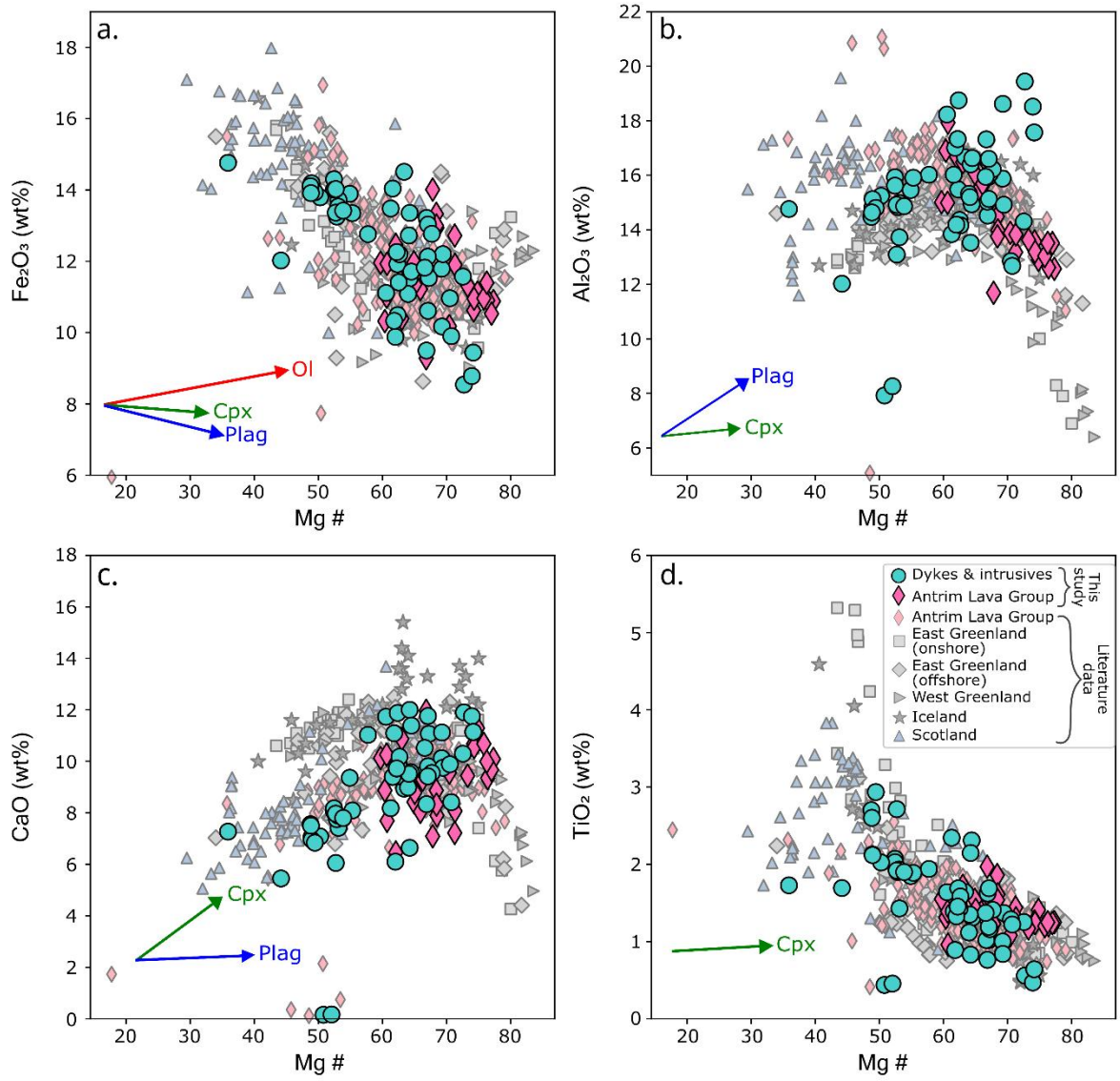

Figure 4: Binary plots showing Mg# versus major elements a) Fe_2O_3, b) Al_2O_3, c) CaO and d) TiO_2. New data in this study are coloured and literature data from the ALG and other NAIP centres are in grey (see legend). Arrows show trajectories towards mineral compositions from Pearson et al. (2003): Ol = olivine, Cpx = clinopyroxene, Plag = plagioclase. Literature data is from genetically related lava flows in Northern Ireland (Carter et al., 2024), the Scottish Hebrides (Hughes et al., 2015c), East Greenland (Philip et al., 2001; Momme et al., 2002), West Greenland (Lightfoot et al., 1997; Keays and Lightfoot, 2007), and Iceland (Momme et al., 2003). 2σ error bars are shown or are less than the size of a data point.

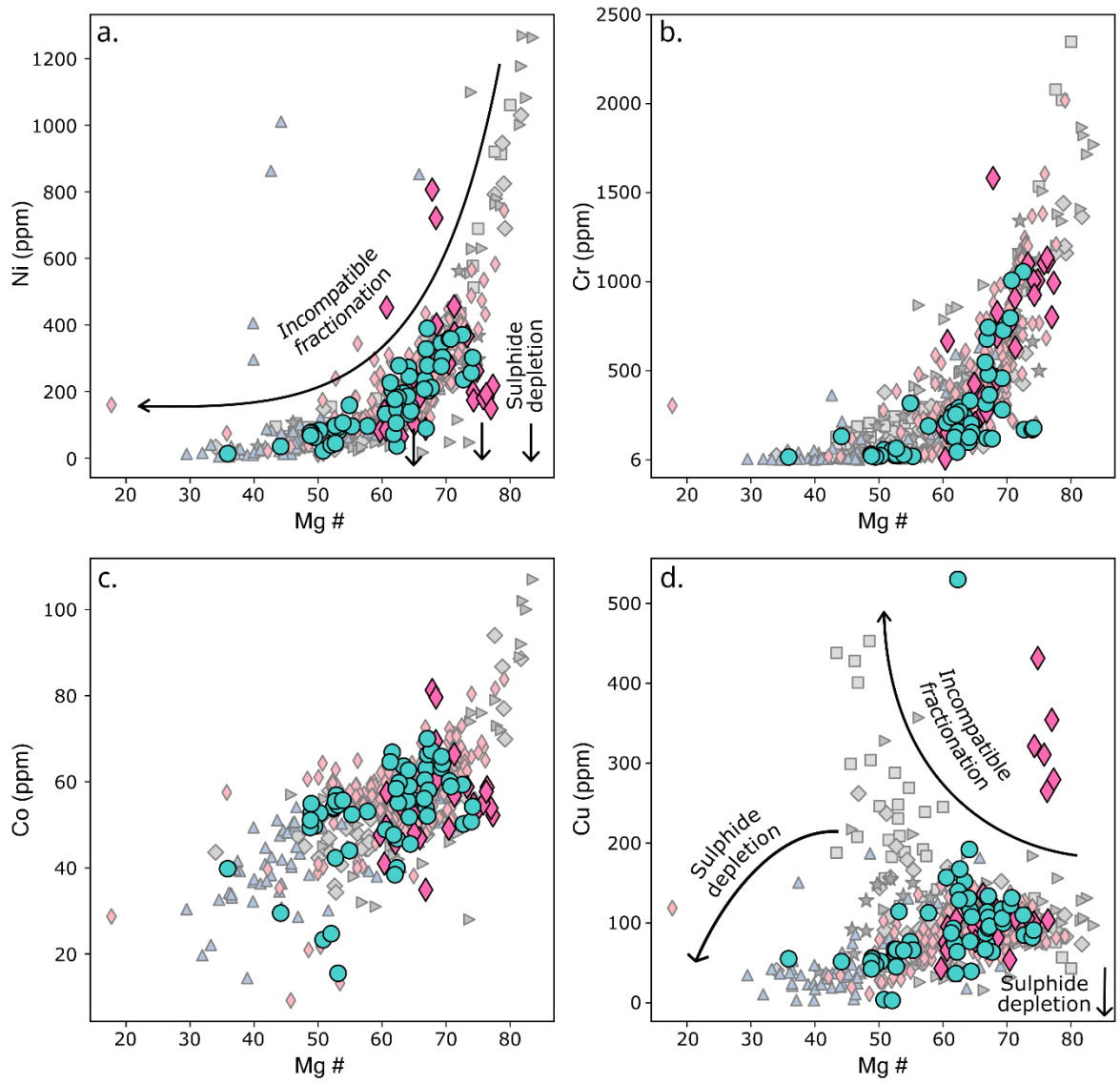

Figure 5: Binary plots showing Mg# versus chalcophile elements a) Ni, b) Cr, c) Co and d) Cu. Schematic Silicate fractionation and sulphide depletion trends are adapted from Hughes et al. (2015c). New data in this study are coloured and literature data from the ALG and other NAIP centres are in grey. See legend and literature data sources in Figure 4. 2σ error bars are shown or are less than the size of a data point.

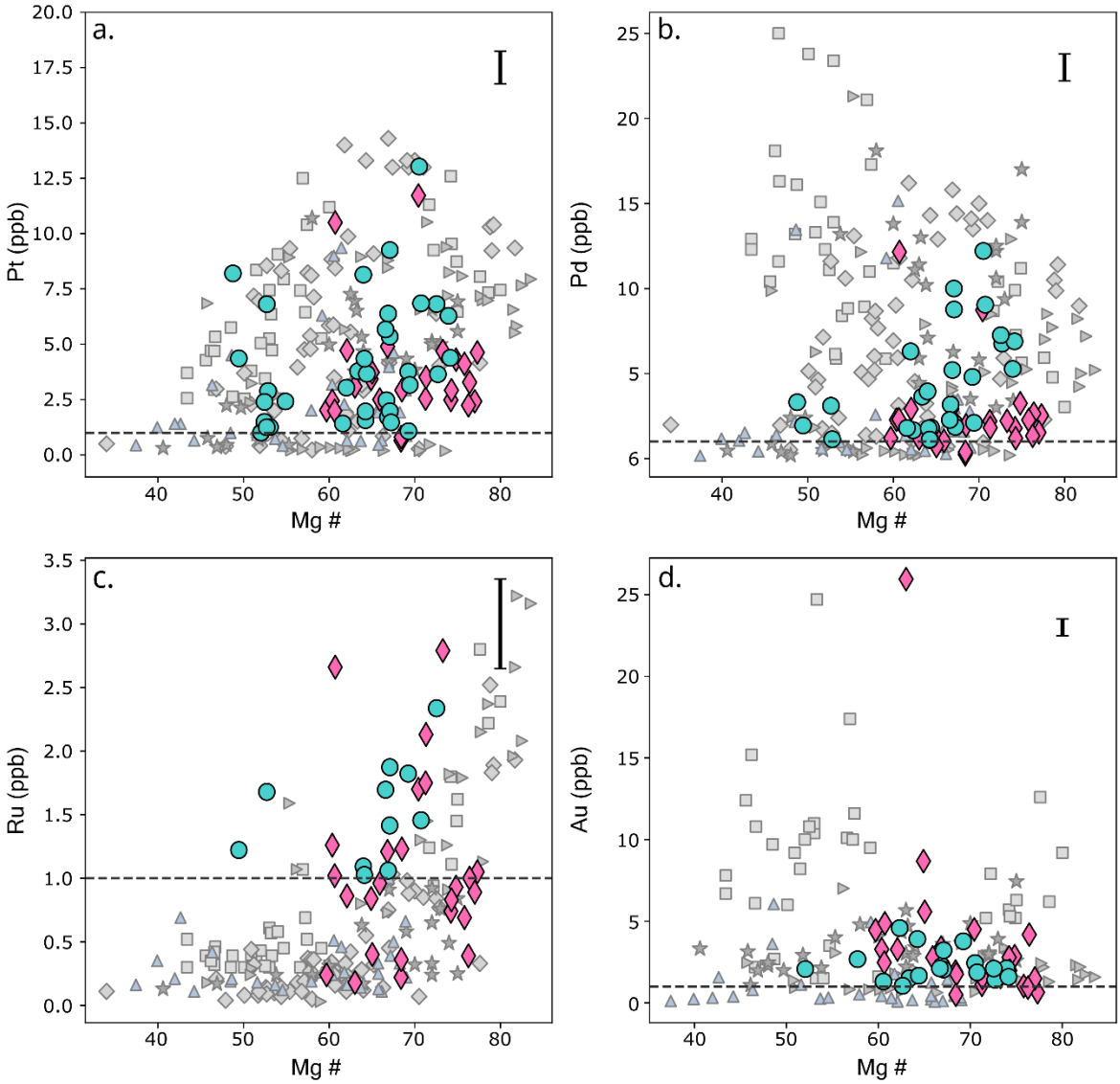

Figure 6: Binary plots showing Mg# versus a) Pt, b) Pd, c) Ru and d) Au. New data in this study are coloured and literature data from the ALG and other NAIP centres are in grey. See legend and literature data sources in Figure 4. 2σ error bars are shown or are less than the size of a data point. The dashed grey line represents the detection limit for dykes and minor intrusions (>1 ppb; Subsets A and B).

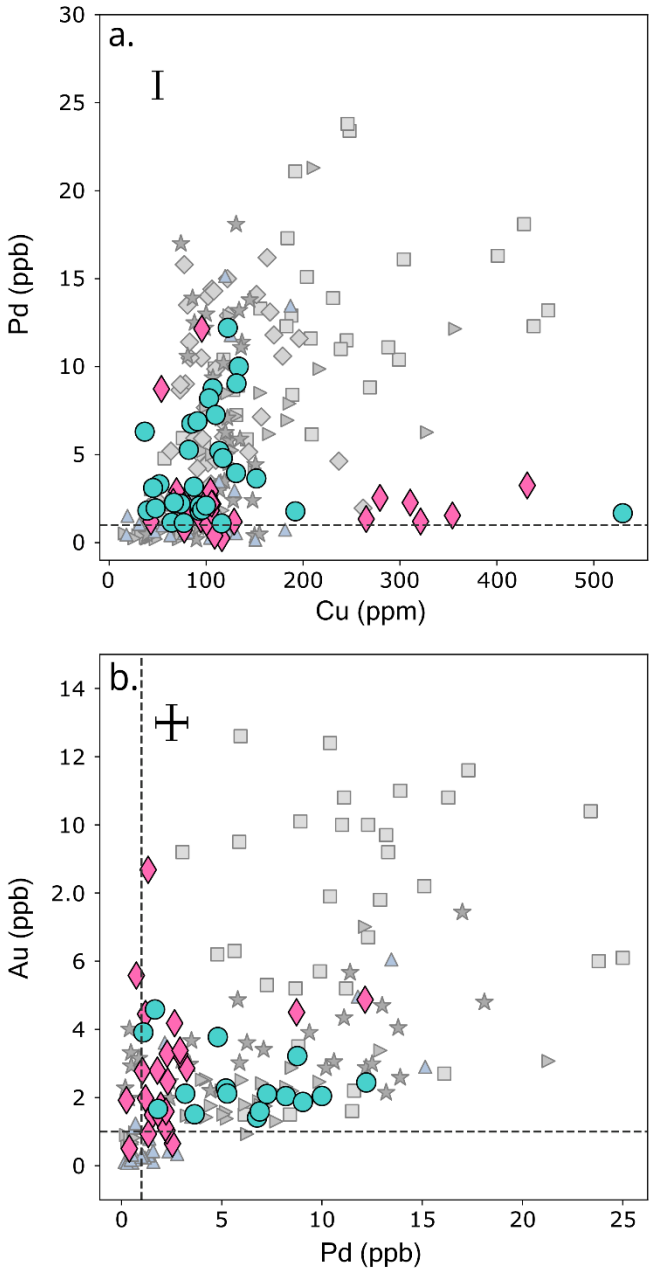

Figure 7: Binary plots showing a) Pd versus Cu and b) Au versus Pd. New data in this study are coloured and literature data from the ALG and other NAIP centres are in grey. See legend and literature data sources in Figure 4. 2σ error bars are shown or are less than the size of a data point. The dashed grey line represents the detection limit for our new dyke and minor intrusion data (>1 ppb; Subsets A and B).

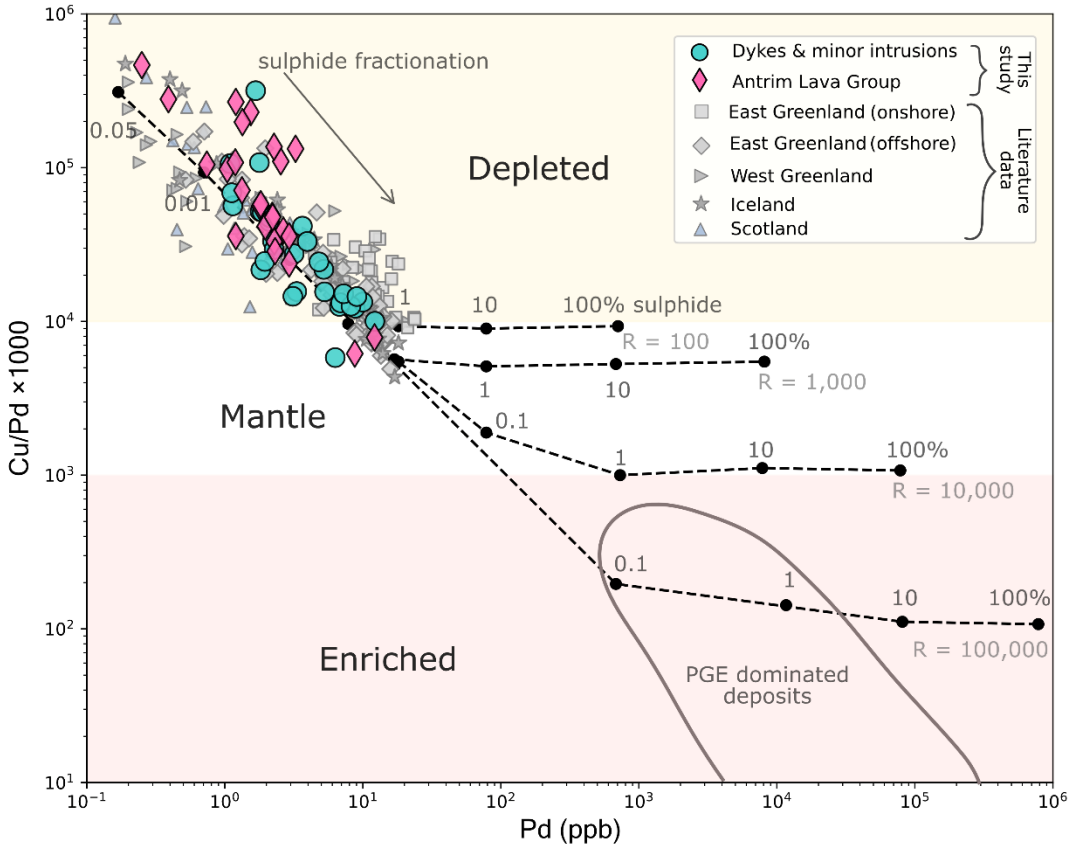

Figure 8: Binary plot showing Cu/Pd ratio versus Pd. The dashed line shows the composition of a modelled basalt melt when a sulphide liquid is added or removed in cotectic proportions. Black points represent composition of rocks containing 0.01, 1, 10% sulphide, R factors describe the mass ratio of silicate melt interacting with a sulphide liquid, and the black polygon shows the composition of samples from major global PGE deposits (e.g. Merensky reef, Bushveld UG-2, Stillwater J-M reef). Adapted from Barnes et al. (1993) and Hughes et al. (2015c). The depleted field (yellow) shows magma compositions with Cu/Pd ratios higher than that of the mantle and are depleted in Pd relative to Cu as sulphide liquids have been exsolved. The enriched field (pink) represents magma compositions with Cu/Pd ratios lower than that of mantle ratios, with Pd enriched relative to Cu as a result of concentration within sulphides. A schematic sulphide fractionation trend has been adapted from Singh et al. (2018). See legend and literature data sources in Figure 4.

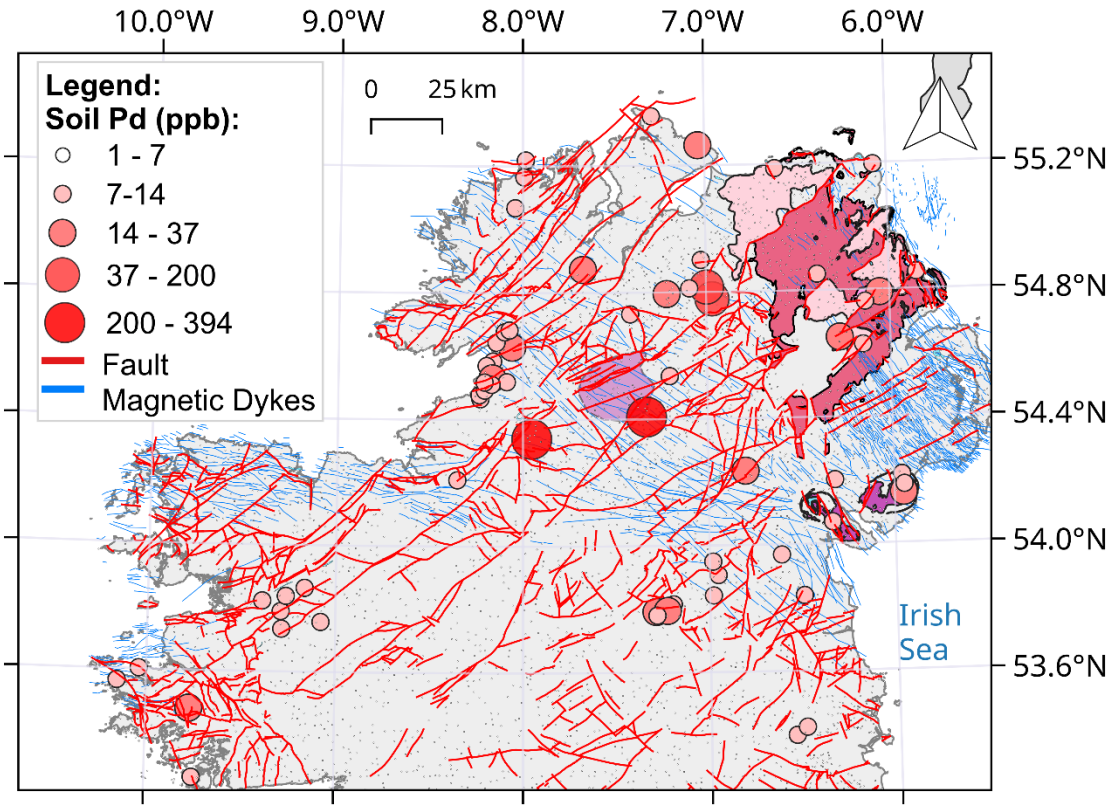

Figure 9: Pd concentrations in deeper topsoils in the Tellus geochemical survey (see Supplementary Text for national datasets). Dykes from our new regional mapping are depicted as blue lines and geological faults are in red. Bedrock geology (ALG, Slieve Gullion, Carlingford, Mourne Mountains, Dromore High) are as in Figure 3a.

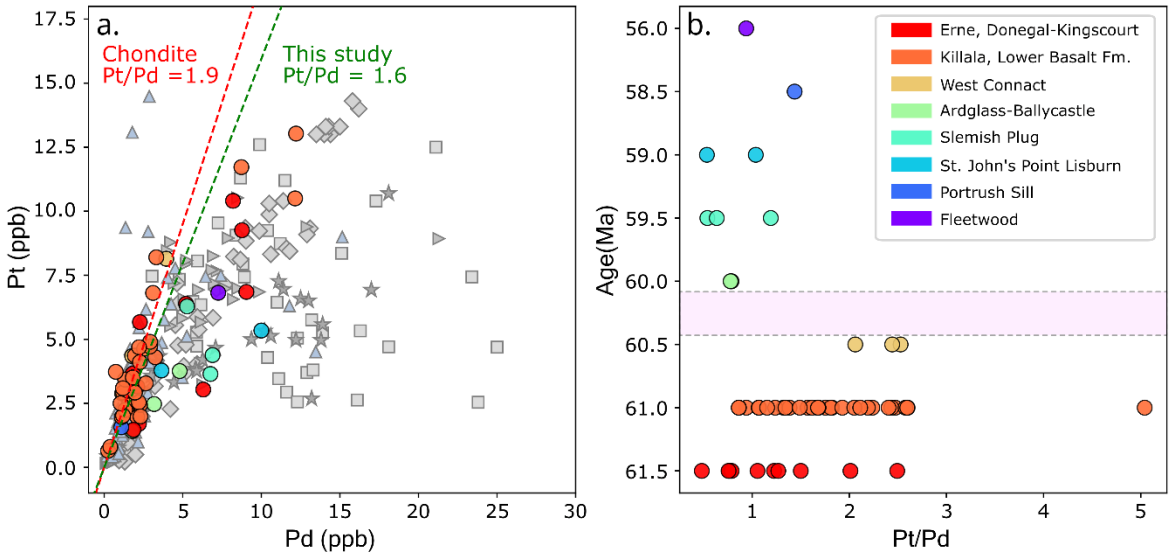

Figure 10: a) Binary plot showing Pt versus in NAIP samples. Undepleted mantle contains approximately chondritic PGE proportions (Carlson, 2005) and comparing samples to chondritic values therefore provides insight into the mantle PGE source enrichment. Samples in this study are in colour (see legend Fig. 10b) and other NAIP centres in grey (see legend and data sources in Figure 4). b) Pt/Pd ratios of samples in this study versus eruption/emplacement time from 61.5-56 Ma. Older samples (before or contemporaneous with the LBF; Cooper et al., 2026) are represented in red-orange and younger samples (after or contemporaneous with the UBF) are represented in blue-purple. Shaded pink area denotes the interbasaltic period hiatus (Carter et al., 2024).

TABLES

Sample	Sample material/dyke swarm	Sample subgroup	Easting	Northing
A1007507	Erne	B	275396	329861
A1007505	Donegal-Kingscourt	B	287267	324574
A1007506	Donegal-Kingscourt	B	286630	324732
MRC404	Donegal-Kingscourt	A	219476	356499
MRC407	Erne	A	244329	354599
MRC462	St. John's Point Lisburn	A	323705	367595
MRC464	St. John's Point Lisburn	A	352760	333317
MRC467	Scrabo Sill	A	347890	372416
MRC471	Fairhead Sill	A	317616	442690
MRC472	Ardglass-Ballycastle	A	324243	425872
MRC475	Ardglass-Ballycastle	A	330388	377893
MRC482	Ardglass-Ballycastle	A	335617	381079
MRC483	Erne	A	244329	354599
MRC496	Fleetwood	A	336090	326710
MRC507	Donegal-Kingscourt	A	174979	373231
MRC510	Killala	A	111404	341170
MRC513	Killala	A	128560	330528
MRC517	Donegal-Kingscourt	A	305557	322080
MRC521	Portrush Sill	A	285600	441400
MRC523	Slemish Plug	A	322400	405700
MRC558	Donegal-Kingscourt	A	307017	339585
MRC574	St. John's Point Lisburn	A	315788	347482
MRC607	Magilligan Sill	A	268300	435300
MRC612	Slemish Plug	A	322099	405469
MRC613	Slemish Plug	A	321969	405488
22CCCI.35	Carlingford Cone Sheet	B	314162	307791
22CCI.23	Carlingford Cone Sheet	B	318325	309050
22CCI.6	Carlingford Cone Sheet	B	313032	313769
MRC622	Fleetwood	A	352405	371156
MRC490	Ardglass-Ballycastle	A	345600	402600
MRC552	Donegal-Kingscourt	A	306637	340314
24-PM-01	West Connacht	B	054400	267200
24-PM-02	West Connacht	B	054200	267400
24-PM-04	West Connacht	B	098200	281800
24-PM-05	West Connacht	B	081100	263500
24-WIT-01	Dingle	B	054237	0452370
24-WIT-02	Dingle	B	054237	0452370
24-WIT-04	Dingle	B	052447	042336
24-WIT-08	West Connacht	B	058805	253276
24-WIT-10	West Connacht	B	054285	257158
24-WIT-12	West Connacht	B	082549	272496
24-WIT-14	West Connacht	B	076934	268576

24-WIT-15	West Connacht	B	075542	267469
24-WIT-16	West Connacht	B	087842	277133
24-WIT-17	West Connacht	B	094896	280295
24-WIT-18	West Connacht	B	094893	280302
24-WIT-19	Killala	B	099368	341768
24-WIT-20	Killala	B	122313	333160
24-WIT-21	Killala	B	122321	333119
24-WIT-22	Killala	B	122335	332890
24-WIT-23	Killala	B	128609	330399
24-WIT-25	Killala	B	128584	330514
24-WIT-28	Killala	B	128522	331092
24-WIT-29	Killala	B	120449	338152
24-WIT-30d	Donegal-Kingscourt	B	180912	382130
24-WIT-32	Donegal-Kingscourt	B	184921	374462
NIRE-01-08-0006	Lower Basalt	C	309473	416438
NIRE-03/08-0004	Lower Basalt	C	332255	414987
NIRE-09/08-0001 (59)	Lower Basalt	C	294362	434582
NIRE-08/08-0002	Lower Basalt	C	295284	417562
NIRE-01/08-0003	Lower Basalt	C	309689	421897
NIRE-03/14-0001	Lower Basalt	C	314741	403813
NIRE-11/08-0001	Lower Basalt	C	287917	413754
NIRE-02/08-0001	Lower Basalt	C	316129	412540
NIRE-03/08-0003	Lower Basalt	C	332828	414530
NIRE-03/08-0002	Lower Basalt	C	333053	414144
NIRE-01/08-0005	Lower Basalt	C	308528	416359
NIRE-04/08-0002	Lower Basalt	C	277179	415701
NIRE-01/08-0002	Lower Basalt	C	302489	419822
NIRE-09/08-0001 (120)	Lower Basalt	C	294362	434582
NIRE-03/08-0001	Lower Basalt	C	326391	406143
MBC49	Lower Basalt	C	297230	425100
NIRE-05/08-0002	Lower Basalt	C	278240	430729
NIRE-04/08-0001	Lower Basalt	C	277233	415430
NIRE-08/08-0001	Lower Basalt	C	296903	417587

Table 1: Details of samples analysed in this study, including the type of igneous material sampled, subgroup classification and sampling GPS location.

Source	GSNI	Fieldwork	Cardiff Research Group
Subgroup	A	B	C
Sample Type	Dykes, sills, plugs	Dykes, cone sheets	Lavas
Location	Counties Antrim, Armagh, Derry, Donegal, Down, Fermanagh, Mayo, Sligo, Tyrone	Counties Cork, Donegal, Galway, Kerry, Louth, Mayo, Monaghan, Sligo	County Antrim
Sample Preparation	Centre for Environmental Geochemistry, Nottingham	Discipline of Geology, Trinity College Dublin; Earth Surface Research Laboratory, Trinity College Dublin	School of Earth and Environmental Sciences, Cardiff University
Major elements	Panalytical Zetium Wavelength Dispersive-Xray Florescence spectroscopy	Panalytical Zetium Wavelength Dispersive X-ray Fluorescence spectrometer	JY-Horiba Ultima 2 Inductively Coupled Plasma Optical Emission Spectrometry
Trace elements	Agilent 7500 Ionising Coupled Plasma-Mass Spectroscopy (ICP-MS)		Thermoelemental X series (X7) ICP-MS
Standards	JG1a, JG3, BE-N, GXR-1, BCR-2, AMIS 0498, OREAS 13b	GSJ JB-1b, JB-3a, JBb-1, GSJ JA-1a, JA-2, JB-2, AMIS 0498, OREAS 13b	JB1a, JP1, MRG1
PGE and Au	Nickel sulphide fire assay followed by ELAN 9000/ thermoelemental X7 ICP-MS		
PGE analytical laboratory	Activation Laboratories Ltd, Canada		School of Earth and Environmental Sciences, Cardiff University
Analytical method details	Hollis et al. (2015), Hoffman and Dunn (2002)	Carter et al. (2024), Hoffman and Dunn (2002)	McDonald and Viljoen (2006), Huber et al. (2001)

Table 2: Summary of analysis methods used for each sample subgroup in this study.

REFERENCES

Á HORNI, J., HOPPER, J. R., BLISCHKE, A., GEISLER, W. H., STEWART, M., MCDERMOTT, K., JUDGE, M., ERLENDSSON, Ö. & ÁRTING, U. 2017. Regional distribution of volcanism within the North Atlantic Igneous Province. *Geological Society, London, Special Publications,* 447**,** 105–125.

ANDERSEN, J. C. Ø., POWER, M. R. & MOMME, P. 2000. Platinum-Group Elements in the Palaeogene North Atlantic Igneous Province. *The Geology, Geochemistry, Mineralogy and Mineral Beneficiation of PGE,* 54**,** 637–667.

ANDERSEN, J. C. Ø., ROLLINSON, G. K., MCDONALD, I., TEGNER, C. & LESHER, C. E. 2017. Platinum-group mineralization at the margin of the Skaergaard intrusion, East Greenland. *Mineralium Deposita,* 52**,** 929–942.

ANDERSON, H., WALSH, J. J. & COOPER, M. R. 2016. Faults, intrusions and flood basalts: the Cenozoic structure of the north of Ireland. *In:* YOUNG, M. E. (ed.) *Unearthed: impacts of the Tellus surveys of the north of Ireland.* Dublin: Royal Irish Academy.

ANDERSON, H., WALSH, J. J. & COOPER, M. R. 2018. The development of a regional-scale intraplate strike-slip fault system; Alpine deformation in the north of Ireland. *Journal of Structural Geology,* 116**,** 47–63.

ANDERSON, P. E., STEVENSON, C. T., COOPER, M. R., MEIGHAN, I. G., HURLEY, C., REAVY, R. J., INMAN, J. & ELLAM, R. M. 2018. Refined model of incremental emplacement based on structural evidence from the granodioritic Newry igneous complex, Northern Ireland. *Geological Society of America Bulletin. GSA Bulletin*. 130 (5-6): 740-756.

BARNES, S.-J., MAIER, W. D. & ASHWAL, L. D. 2004. Platinum-group element distribution in the Main Zone and Upper Zone of the Bushveld Complex, South Africa. *Chemical Geology,* 208**,** 293–317.

BARNES, S.-J. & MANSUR, E. T. 2022. Distribution of Te, As, Bi, Sb, and Se in Mid-Ocean Ridge Basalt and Komatiites and in Picrites and Basalts from Large Igneous Provinces: Implications

for the Formation of Magmatic Ni-Cu-Platinum Group Element Deposits. *Economic Geology,* 117**,** 1919–1933.

BARNES, S. J., COUTURE, J. F., SAWYER, E. W. & BOUCHAIB, C. 1993. Nickel-Copper occurrences in the BA belt of Pontiac Sub province and the use of Cu-Pd ratios in interpreting PGE distributions. *Economic Geology,* 88**,** 1402–1418.

BARNES, S. J., CRUDEN, A. R., ARNDT, N. & SAUMUR, B. M. 2016. The mineral system approach applied to magmatic Ni–Cu–PGE sulphide deposits. *Ore Geology Reviews,* 76**,** 296–316.

BARNES, S. J., MUNGALL, J. E. & MAIER, W. D. 2015. Platinum group elements in mantle melts and mantle samples. *Lithos,* 232**,** 395–417.

BARNES, S. J. & RIPLEY, E. M. 2016. Highly siderophile and strongly chalcophile elements in magmatic ore deposits. *Reviews in Mineralogy and Geochemistry,* 81**,** 725–74.

BECKWITH, J., STOCK, M.J., HOLNESS, M.B., COOPER, M.R., ANDERSEN, J.C.Ø., HUBER, C., CHEW, D.M., HIGGINS, O., CARTER, E.J., BROOM-FENDLEY, S. 2026. Transient liquid- and solid-dominated inflation of an upper crustal magma chamber: insights from the Carlingford Complex (Ireland), Preprint DOI: https://doi.org/10.31223/X55N1W.

BONADIO, R., LEBEDEV, S., CHEW, D., XU, Y., FULLEA, J. AND MEIER, T. 2025. Volcanism and long-term seismicity controlled by plume-induced plate thinning. *Nature Communications*, *16*(1), p.7837.

CARLSON, R.W., 2005. Application of the Pt–Re–Os isotopic systems tomantle geochemistry and geochronology. Lithos 82, 249–272.

CARTER, E. J., STOCK, M. J., BERESFORD-BROWNE, A., COOPER, M. R., RAINE, R. & FEREYROLLES, A. 2024. Volcanic tempo driven by rapid fluctuations in mantle temperature during large igneous province emplacement. *Earth and Planetary Science Letters,* 644.

CHAMBERS, L.M., PRINGLE, M.S., 2001. Age and duration of activity at the Isle of Mull Tertiary igneous centre, Scotland, and confirmation of the existence of subchrons during Anomaly 26r. Earth and Planetary Science Letters 193, 333–345.

CHEN, C., FORSTER, M. W., SHCHEKA, S. S., EZAD, I. S., SHEA, J. J., LIU, Y., JACOB, D. E. & FOLEY, S. F. 2025. Sulfide-rich continental roots at cratonic margins formed by carbonated melts. *Nature,* 637**,** 615–621.

COOPER, M. R., ANDERSON, H., WALSH, J. J., VAN DAM, C. L., YOUNG, M. E., EARLS, G. & WALKER, A. 2012. Palaeogene Alpine tectonics and Icelandic plume-related magmatism and deformation in Northern Ireland. *Journal of the Geological Society,* 169**,** 29–36.

COOPER, M. R., CROWLEY, Q. G., HOLLIS, S. P., NOBLE, S. R, & HENNEY, P. 2013. A U-Pb age for the Late Caledonian Sperrin Mountains minor intrusions suite in the north of Ireland: timing of slab break-off in the Grampian terrane and the significance of deep-seated, crustal lineaments. *Journal of the Geological Society, London.* 170, 603-614.

COOPER, M. R, CROWLEY, Q. G., HOLLIS, S. P., NOBLE, S. R., ROBERTS, S., CHEW, D. M., MERRIMAN, R. J., EARLS, G. & HERRINGTON, R. 2011. Age constraints and geochemistry of the Ordovician Tyrone Igneous Complex, Northern Ireland: implications for the Grampian orogeny. *Journal of the Geological Society, London, Vol.* 168; p. 837-850. doi: 10.1144/0016-76492010-164.

COOPER, M. R., TAPSTER, S. & CONDON, D. 2020. Feeling the pulse? New high resolution U-Pb zircon geochronological constraints for the Northern Ireland sector of the North Atlantic Igneous Province. *EGU General Assembly 2020.* Online, 4–8 May 2020: EGU2020-8464.

COOPER, M. R., TAPSTER, S. & CONDON, D. 2026 Feeling the pulse? Paleogene chronostratigraphy of Northern Ireland and the north of Ireland temporally coupled to the North Atlantic Igneous Province. *Geology, v. XX, p. XXX–XXX,* https://doi.org/10.1130/G54157.1.

DEWEY, J. F. 2000. Cenozoic tectonics of western Ireland. *Proceedings of the Geologists' Association,* 111**,** 291–306.

DICKIN, A.P. AND DURANT, G.P., 2002. The Blackstones Bank igneous complex: geochemistry and crustal context of a submerged Tertiary igneous centre in the Scottish Hebrides. *Geological Magazine*, *139* (2), pp.199-207.

GAGNEVIN, D., HAUGHTON, P. D., WHITING, L. & SAQQB, M. M. 2018. Geological and geophysical evidence for a mafic igneous origin of the porcupine arch, offshore Ireland. *Journal of the Geological Society,* 175**,** 210–228.

GEOFFROY, L., BERGERAT, F. & ANGELIER, J. 1996. Brittle tectonism in relation to the Palaeogene evolution of the Thulean/NE Atl domain: a study in Ulster. *Geological Journal,* 31**,** 259–269.

GOODMAN, R. & SLOWLEY, E. 2005. Independent review of exploration interests of BelmoreResources Ltd.

GRIFFIN, W. L., BEGG, G. C. & O'REILLY, S. Y. 2013. Continental-root control on the genesis of magmatic ore deposits. *Nature Geoscience,* 6**,** 905–910.

GROUP ELEVEN CORP. 2020. Group Eleven Identifies Anomalous Palladium, Nickel and Cobalt at Ballinalack Zinc Project, Ireland. Vancouver, Canada.

HANSEN, J., JERRAM, D. A., MCCAFFREY, K. & PASSEY, S. R. 2009. The onset of the North Atlantic Igneous Province in a rifting perspective. *Geological Magazine,* 146**,** 309–325.

HAO, H., CAMPBELL, I. H., ARCULUS, R. J. & PERFIT, M. R. 2021. Using precious metal probes to quantify mid-ocean ridge magmatic processes. *Earth and Planetary Science Letters,* 553.

HOFFMAN, E. L. & DUNN, B. 2002. Sample preparation and bulk analytical methods for PGE. *The Geology, Geochemistry, Mineralogy and Mineral Beneficiation of PGE,* 54**,** 1–11.

HOLLIS, S.P., COOPER, M.R., HERRINGTON, R.J., ROBERTS, S., EARLS, G., VERBEETEN, A.,PIERCEY, S.J., AND ARCHIBALD, S.M. 2015. Distribution, mineralogy and geochemistry of silica-iron exhalites and related rocks from the Tyrone Igneous Complex: Implications for VMS mineralization in Northern Ireland. *Journal of Geochemical Exploration* 159: 148-168.

HOLNESS M.B., GEIFMAN E., STOCK M.J., COOPER M.R., BECKWITH J., HUBER C., CHEW D., AND ANDERSEN J.C.Ø., 2025. A microstructural investigation of the Portrush Sill, County Antrim, Northern Ireland: constraints on sill thickness and evidence for crustal assimilation. Lithos.

HUBER, H., KOEBERL, C., MCDONALD, I., REIMOND,W.U., 2001. Geochemistry and petrology of Witwatersrand and Dwyka diamictites from South Africa: search for an extraterrestrial component. Geochimica et Cosmochimica Acta 65, 2007–2016.

HUGHES, H. S. R. 2015. *Temporal, lithospheric and magmatic process controls on ni, cu and platinum-group element (pge) mineralisation: A case study from scotland.* Doctoral Thesis, Cardiff University.

HUGHES, H. S. R., BOYCE, A. J., MCDONALD, I., DAVIDHEISER-KROLL, B., HOLWELL, D. A., MCDONALD, A. & OLDROYD, A. 2015a. Contrasting mechanisms for crustal sulphur contamination of mafic magma: evidence from dyke and sill complexes from the British Palaeogene Igneous Province. *Journal of the Geological Society,* 172**,** 443–458.

HUGHES, H. S. R., MCDONALD, I., BOYCE, A. J., HOLWELL, D. A. & KERR, A. C. 2016. Sulphide Sinking in Magma Conduits: Evidence from Mafic–Ultramafic Plugs on Rum and the Wider North Atlantic Igneous Province. *Journal of Petrology,* 57**,** 383–416.

HUGHES, H. S. R., MCDONALD, I., FAITHFULL, J. W., UPTON, B. G. J. & DOWNES, H. 2015b. Trace-element abundances in the shallow lithospheric mantle of the North Atlantic Craton margin: Implications for melting and metasomatism beneath Northern Scotland. *Mineralogical Magazine,* 79**,** 877–907.

HUGHES, H. S. R., MCDONALD, I., GOODENOUGH, K. M., CIBOROWSKI, T. J. R., KERR, A. C., DAVIES, J. H. F. L. & SELBY, D. 2014. Enriched lithospheric mantle keel below the Scottish margin of the North Atlantic Craton: Evidence from the Palaeoproterozoic Scourie Dyke Swarm and mantle xenoliths. *Precambrian Research,* 250**,** 97–126.

HUGHES, H. S. R., MCDONALD, I. & KERR, A. C. 2015c. Platinum-group element signatures in the North Atlantic Igneous Province: Implications for mantle controls on metal budgets during continental breakup. *Lithos,* 233**,** 89–110.

HURST, E. 1997. Renewal Report for Prospecting Licence 3843. BHP.

KEAYS, R. R. & LIGHTFOOT, P. C. 2007. Siderophile and chalcophile metal variations in Tertiary picrites and basalts from West Greenland with implications for the sulphide saturation history of continental flood basalt magmas. *Mineralium Deposita,* 42**,** 319–336.

KENT, R. W. & FITTON, J. G. 2000. Mantle sources and melting dynamics in the British Palaeogene Igneous Province. *Journal of Petrology,* 41**,** 1023–1040.

KERR, A.C., KENT, R.W., THOMSON, B.A., SEEDHOUSE, J.K. AND DONALDSON, C.H., 1999. Geochemical evolution of the Tertiary Mull volcano, western Scotland. *Journal of Petrology*, *40*(6), pp.873-908.

LE BAS, M.J., LE MAITRE, R.W., STRECKEISEN, A., & ZANETTIN, B. 1986. A chemical classification of volcanic rocks based on the total alkali–silica diagram. *Journal of Petrology*, 27(3), 745–750. https://doi.org/10.1093/petrology/27.3.745

LIGHTFOOT, P. C., HAWKESWORTH, C. J., OLSHEFSKY, K., GREEN, T., DOHERTY, W. & KEAYS, R. R. 1997. Geochemistry of Tertiary tholeiites and picrites from Qeqertarssuaq (Disko Island) and Nuussuaq, West Greenland with implications for the mineral potential of comagmatic intrusions. *Contributions to Mineralogy and Petrology,* 128**,** 139–163.

LINDSAY, J. J., HUGHES, H. S. R., SMYTH, D., MCDONALD, I., BOYCE, A. J. & ANDERSEN, J. C. Ø. 2018. Distinct sulfur saturation histories within the Palaeogene Magilligan Sill, Northern Ireland: implications for Ni – Cu – platinum group element mineralisation in the North Atlantic Igneous Province. *Canadian Journal of Earth Sciences,* 56**,** 774–789.

LINDSAY, J. J., HUGHES, H. S. R., YEOMANS, C. M., ANDERSEN, J. C. Ø. & MCDONALD, I. 2021. A machine learning approach for regional geochemical data: Platinum-group element geochemistry vs geodynamic settings of the North Atlantic Igneous Province. *Geoscience Frontiers,* 12.

LONMIN PLC. 2018. Mineral Resource and Mineral Reserve Statement 2018. London. UK.

LUSTY, P. A. J. 2016. Critical metals for hightechnology applications: mineral exploration potential in the north of Ireland. *In:* YOUNG, M. E. (ed.) *Unearthed: impacts of the Tellus surveys of the north of Ireland.* Dublin: Royal Irish Academy.

LYLE, P. & PRESTON, J. 1993. Geochemistry and volcanology of the Tertiary basalts of the Giant's Causeway area, Northern Ireland. *Journal of the Geological Society,* 150**,** 109–120.

MACDONALD, R., BAGIŃSKI, B., UPTON, B. G. J., PINKERTON, H., MACINNES, D. A. & MACGILLIVRAY, J. C. 2018. The Mull Palaeogene dyke swarm: insights into the evolution of the Mull igneous centre and dyke-emplacement mechanisms. *Mineralogical Magazine,* 74**,** 601–622.

MAIER, W. D. 2005. Platinum-group element (PGE) deposits and occurrences: Mineralization styles, genetic concepts, and exploration criteria. *Journal of African Earth Sciences,* 41**,** 165–191.

MAIER, W.D., GROVES, D.I., 2011. Temporal and spatial controls on the formation of magmatic PGE and Ni–Cu deposits. Mineralium Deposita 46, 841–857.

MCDONALD, I., VILJOEN, K.S., 2006. Platinum-group element geochemistry of mantle eclogites: a reconnaissance study of xenoliths from the Orapa kimberlite, Botswana. Applied Earth Science 115, 81–93.

MITCHELL, W. (ed.) 2004. *Geology of Northern Ireland: our natural foundation*: Geological Survey of Northern Ireland.

MOHR, P. 1988. The Analcime-Olivine Dolerites of West Connacht, Ireland: Classification and Genetic. *Irish Journal of Earth Sciences,* 9**,** 133–140.

MOHR, P. 2000. Late Palaeozoic and Palaeocene magmatic intrusion levels in West Connacht and inferences for palaeotopography. *Proceedings of the Geologists' Association,* 111**,** 337–343.

MOMME, P., ÓSKARSSON, N. & KEAYS, R. R. 2003. Platinum-group elements in the Icelandic rift system: melting processes and mantle sources beneath Iceland. *Chemical Geology,* 196**,** 209–234.

MOMME, P., TEGNER, C., BROOKS, K. C. & KEAYS, R. R. 2002. The behaviour of platinum-group elements in basalts from the East Greenland rifted margin. *Contributions to Mineralogy and Petrology,* 143**,** 133–153.

MORRIS, P. 1974. A Tertiary Dyke System in South-West Ireland. *Proceedings of the Royal Irish Academy. Section B: Biological, Geological and Chemical Science,* 74**,** 179–184.

MUDD, G. M., JOWITT, S. M. & WERNER, T. T. 2018. Global platinum group element resources, reserves and mining - A critical assessment. *Sci Total Environ,* 622-623**,** 614–625.

MUSSETT, A. E., DAGLEY, P. & SKELHORN, R. R. 1988. Time and duration of activity in the British Tertiary Igneous Province. *Geological Society, London, Special Publications,* 39**,** 337–348.

NALDRETT, A.J., 1999. World-class Ni-Cu-PGE deposits: key factors in their genesis. *Mineralium deposita*, *34*(3), pp.227-240.

O'CONNOR, J.M., STOFFERS, P., WIJBRANS, J.R., SHANNON, P.M. AND MORRISSEY, T., 2000. Evidence from episodic seamount volcanism for pulsing of the Iceland plume in the past 70 Myr. *Nature*, *408* (6815), pp.954-958.

PASSMORE, E. 2009. *Feeding large eruptions: crystallisation, mixing and degassing in Icelandic magma chambers.* Doctoral Thesis, University of Edinburgh.

PEARSON, D.G., CANIL, D. AND SHIREY, S.B., 2003. Mantle samples included in volcanic rocks: xenoliths and diamonds. *Treatise on geochemistry*, *2*, p.568.

PHILIP, H., ECKHARDT, J. D. & PUCHELT, H. 2001. Platinum-group elements (PGE) in basalts of the seaward-dipping reflector sequence, SE Greenland coast. *Journal of Petrology,* 42**,** 407–432.

PRESTON, J. 1963. The Dolerite plug at Slemish, Co Antrim, Ireland. *Geological Journal,* 3**,** 301–314.

REAY, D.M., 2004. Chapter 22, Oil and Gas. in Mitchell, W.I. ed. The Geology of Northern Ireland - Our Natural Foundation (second edition): Belfast, Geological Survey of Northern Ireland, p. 273–290.

RITCHIE, J. D. & HITCHEN, K. 1996. Early Paleogene offshore igneous activity to the northwest of the UK and its relationship to the North Atlantic Igneous Province. *Geological Society, London, Special Publications,* 101**,** 63–78.

SAUNDERS, A. D., FITTON, J. G., KERR, A. C., NORRY, M. J. & KENT, R. W. 1997. The North Atlantic Igneous Province. *Large Igneous Provinces: Continental, Oceanic, and Planetary Flood Volcanism,* 100**,** 45–93.

SAUNDERS, A. D., LARSEN, H. C. & FITTON, J. G. 1998. Magmatic development of the southeast Greenland Margin and evolution of the Iceland plume: geochemical constraints from Leg 152. *Proceedings of the Ocean Drilling Program, Scientific Results,* 152**,** 479–501.

SINGH, T. D., MANIKYAMBA, C., SUBRAMANYAM, K. S. V., GANGULY, S., KHELEN, A. C. & RAMAKRISHNA REDDY, N. 2018. Mantle heterogeneity, plume-lithosphere interaction at rift controlled ocean-continent transition zone: Evidence from trace-PGE geochemistry of Vempalle flows, Cuddapah Basin, India. *Geoscience Frontiers,* 9**,** 1809–1827.

SHAW, J.I., TORVELA, T., COOPER, M.R, LESLIE, A.G., CHAPMAN, R.J., 2022. A progressive model for the development of the Cavanacaw Au–Ag–Pb vein deposit, Northern Ireland, and implications for the evolution and metallogeny of the Grampian Terrane. Journal of Structural Geology, 161. 104637. ISSN 0191-81

SMYTH, D. 2014. Lonmin Plc exploration in Northern Ireland – the contribution of mineral exploration to new observations in regional geology. *Mineral Deposits Studies Group 38th Annual Meeting,* Univeristy of Southampton.

WILKINSON, C. M., GANERØD, M., HENDRIKS, B. W. H. & EIDE, E. A. 2016. Compilation and appraisal of geochronological data from the North Atlantic Igneous Province (NAIP). *Geological Society, London, Special Publications,* 447**,** 69–103.

SUPPLEMENTARY MATERIAL

SUPPLEMENTARY TABLES

Table S1: Total Sulphur content for subgroup A samples.

Table S2: Analytical and preparation accuracy and reproducibility assessment.

Table S3: Major Element analysis results for all samples in this study.

Table S4: Trace element analysis results for all samples in this study.

Table S5: PGE + Au analysis results for all samples in this study.

SUPPLEMENTARY TEXT

National dataset reference list

BRITISH GEOLOGICAL SURVEY. 2008. *BGS Geology 625k*. [dataset] British Geological Survey. Available at: https://www.bgs.ac.uk/datasets/bgs-geology-625k/.

GEOLOGICAL SURVEY OF IRELAND. 2021. *Bedrock Geology 1:100,000 Ireland (ROI) ITM*. Dublin: Geological Survey of Ireland.

GEOLOGICAL SURVEY OF IRELAND. 2022. Tellus Merge-2022 airborne geophysical technical report. Dublin: Geological Survey of Ireland.

GEOLOGICAL SURVEY IRELAND AND GEOLOGICAL SURVEY OF NORTHERN IRELAND (2022) *Tellus geochemical survey: deeper topsoil ('S' horizon) multi-element maps for the northern half of Ireland*. Dublin: Geological Survey Ireland.

GEOLOGICAL SURVEY OF NORTHERN IRELAND (GSNI). 2005. *Tellus Rural Soil Survey: Regional S Soils – Fire Assay dataset*. [dataset] Geological Survey of Northern Ireland (Department for the Economy), Northern Ireland. Available at:

https://admin.opendatani.gov.uk/dataset/rural-soil-survey/resource/e9a4568a-677d-419a-a2ce-31940900bbe9

Certified Reference Material certifications

AMIS 2017. AMIS 0498: Certified Reference Material Platinum (PGM). Platreef Ore Bushveld Complex, South Africa. Certificate of Analysis Modderfontein, South Africa: A Division of Torre Analytical Services (Pty) Limited.

GEOLOGICAL SURVEY OF JAPAN (GSJ) (2024) *Geochemical Reference Standards Database*. Available at: https://gbank.gsj.jp/geostandards/welcome.html.

GLADNEY, E.S., ROELANDTS, I., & GILLS, T.E. (1988) '1988 Compilation of elemental concentration data for CCRMP reference rock samples SY-2, SY-3, and MRG-1', *Geostandards and Geoanalytical Research*, 14(3), pp. 373–458. doi:10.1111/j.1751-908X.1990.tb00078.x.

GOUVEIA, M.A., PRUDÊNCIO, M.I., BARROS, J.S., MORGADO, L. AND CABRAL, J.M.P., 1994. Elemental concentration data for USGS geochemical exploration reference materials GXR-1 to GXR-4 and GXR-6. *Journal of radioanalytical and nuclear chemistry*, *179*(1), pp.165-172.

NIST 2014. Certificate of Analysis: Standard Reference Material® 2684c *In:* GONZALEZ, C. A. (ed.) *Bituminous Coal (Nominal Mass Fraction 3 % Sulfur)* Gaithersburg, MD 20899 National Institute of Standards & Technology.

ORE RESEARCH & EXPLORATION PTY LTD. 2009. Certificate of analysis for PGE-Cu-Ni reference material OREAS 13b Victoria, Australia.

SARM. (2022). *Certificate of analysis: BE-N reference material (basalt)*. Service d'Analyses des Roches et des Minéraux, Centre de Recherches Pétrographiques et Géochimiques (CRPG-CNRS), Vandoeuvre-lès-Nancy, France.

USGS (2022) *BCR-2 Geochemical Reference Material Information Sheet*. United States Geological Survey. Available at: https://www.usgs.gov/media/files/bcr-2-geochemical-reference-material-information-sheet-0

SUPPLEMENTARY FIGURES

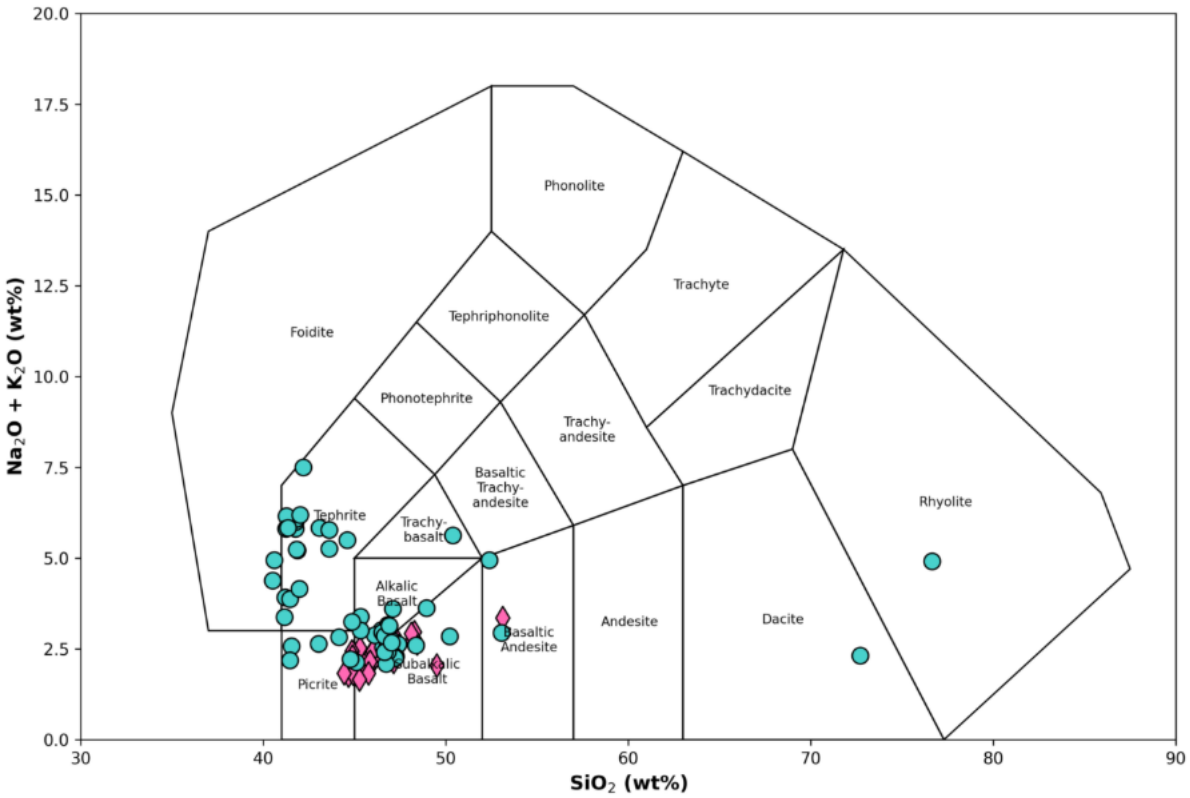

Figure S1: Total Alkali Silica diagram showing the classification of volcanic samples in this study (after Le Bas et al., 1986). See legend and data sources in Fig. 4.

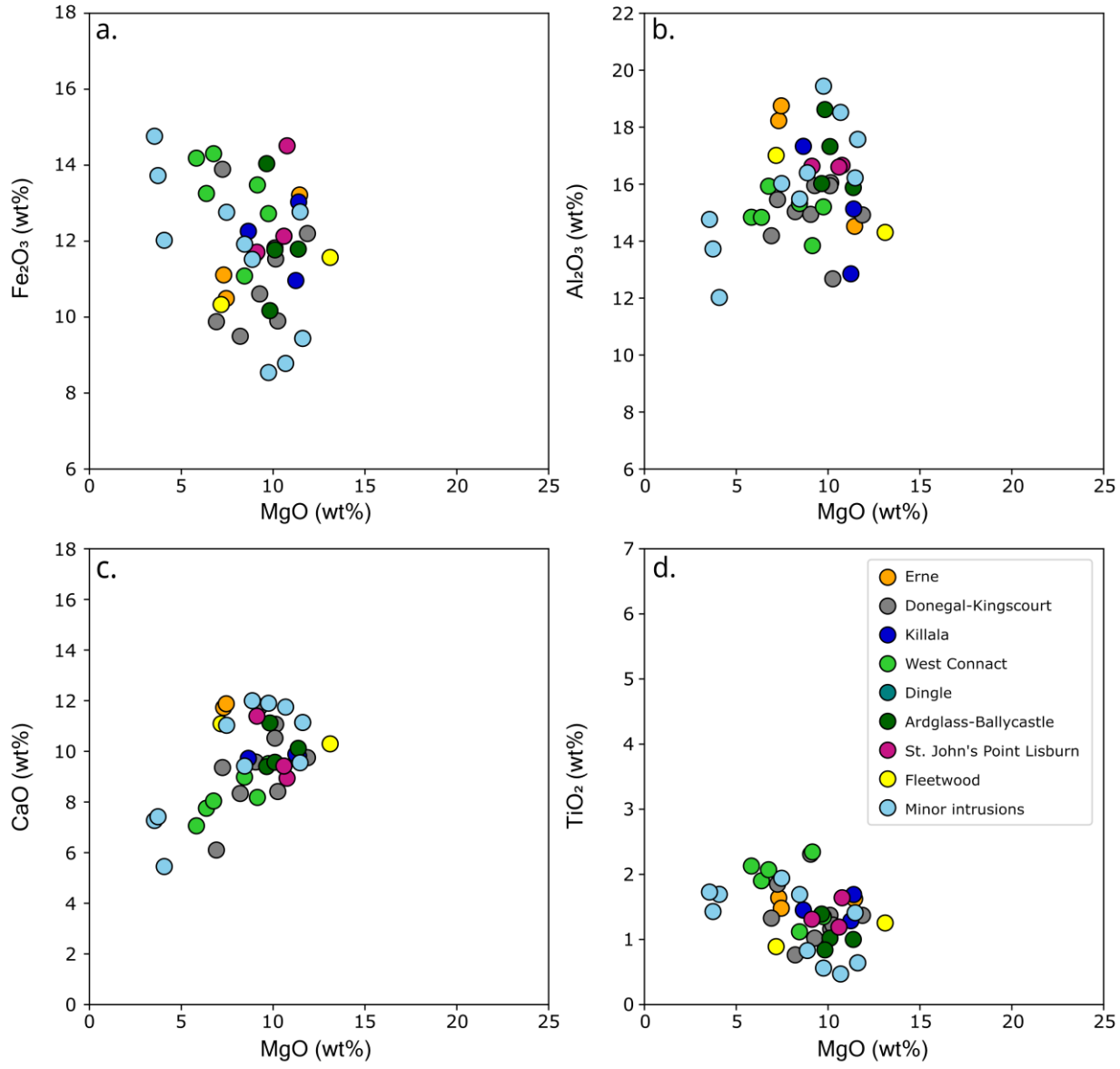

Figure S2: Binary plots showing the major element compositions of intrusive samples analysed in this study with MgO versus a) Fe_2O_3, b) Al_2O_3, c) CaO and d) TiO_2. Dykes are categorised according to swarm (see Fig. 3a). Minor intrusions comprise Portrush sill, Magilligan Sill, Slemish plug and Carlingford cone sheets.

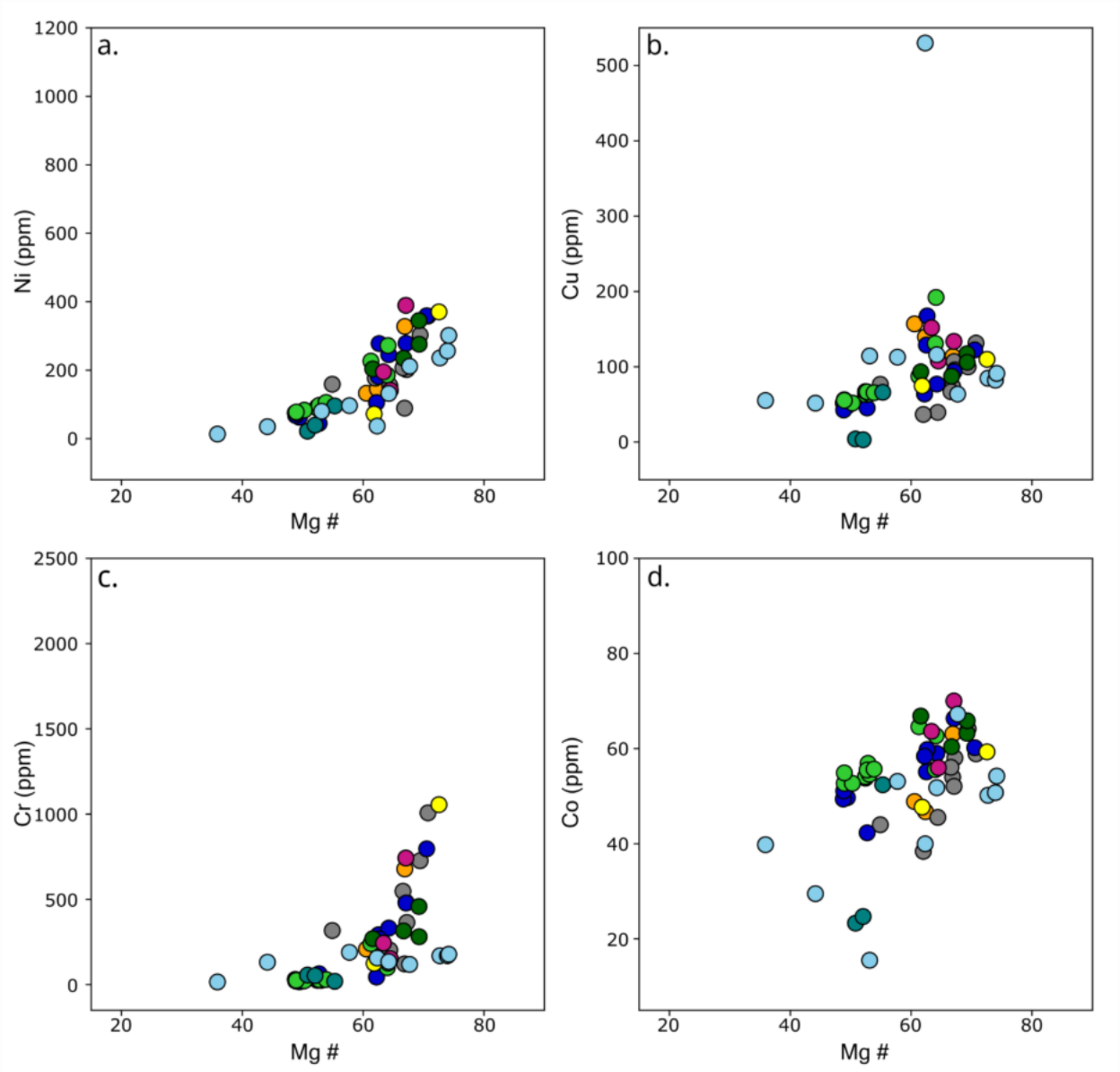

Figure S3: Binary plots showing the chalcophile element compositions of intrusive samples analysed in this study with Mg# versus a) Ni, b) Cu, c) Cr and d) Co. Dykes are categorised according to swarm (see Fig. 3a).

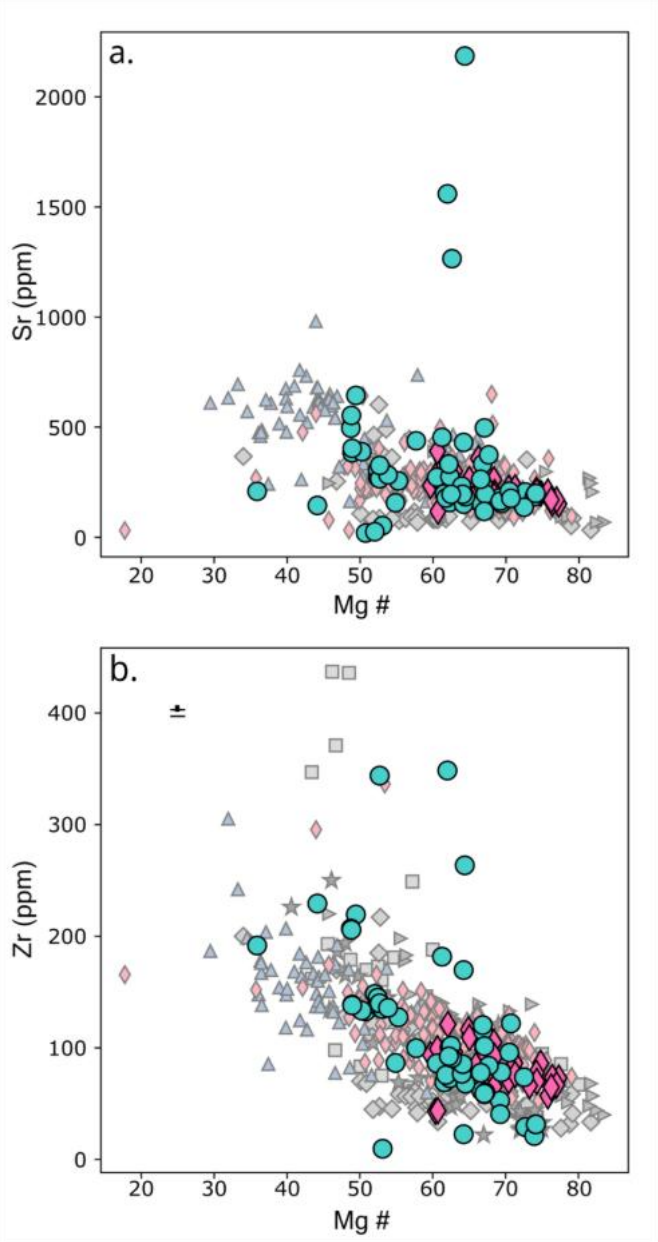

Figure S4: Binary plots showing Mg# versus lithophile trace elements a) Sr and b) Zn. New data in this study are coloured and literature data from the ALG and other NAIP centres are in grey. See legend and literature data sources in Figure 4. 2σ error bars are shown or are less than the size of a data point.